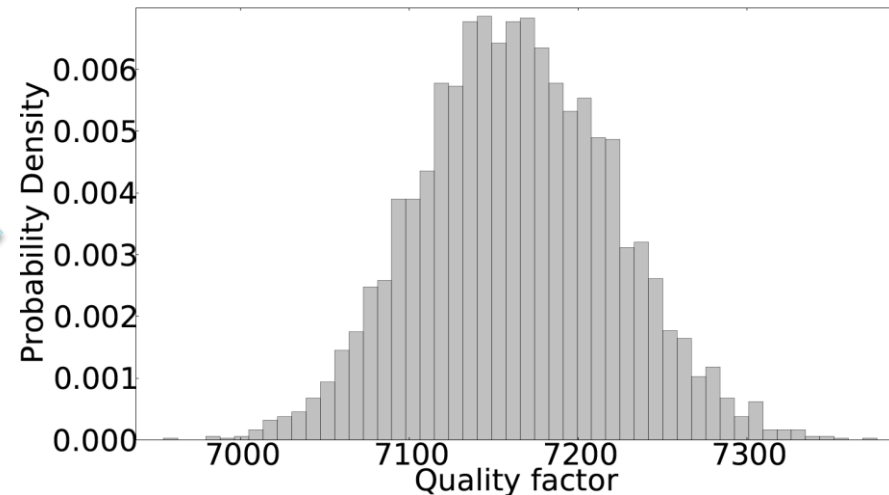
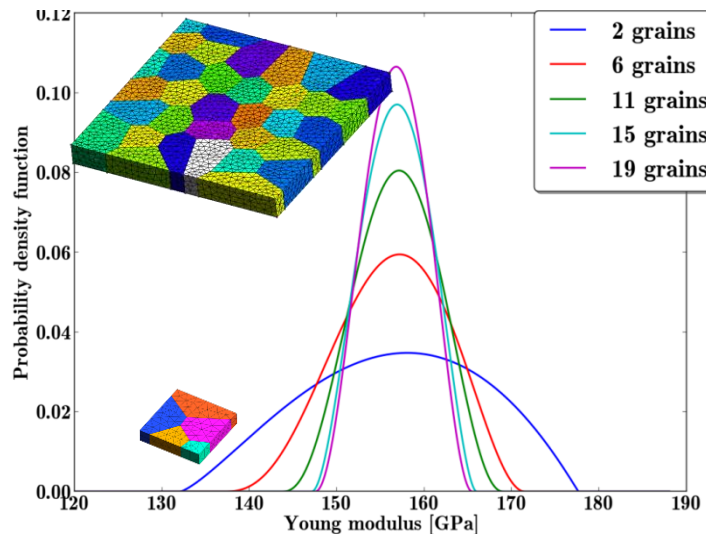


A stochastic 3-Scale approach to study the thermo- mechanical damping of MEMS

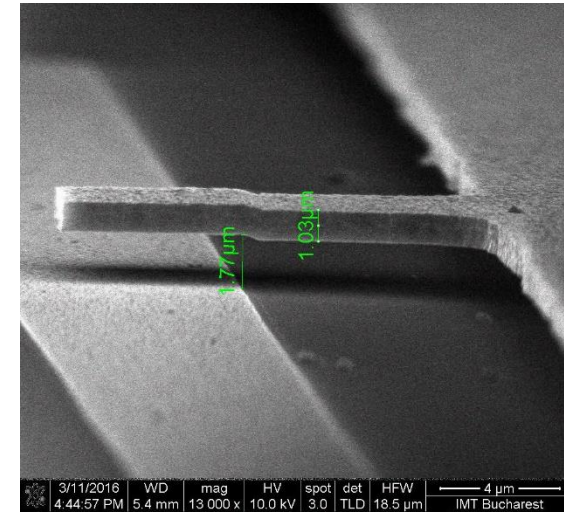
*Wu Ling, Lucas Vincent, Nguyen Van-Dung, Paquay Stéphane,
Golinval Jean-Claude, Noels Ludovic
Voicu Rodica, Baracu Angela, Muller Raluca*



3SMVIB: The research has been funded by the Walloon Region under the agreement no 1117477 (CT-INT 2011-11-14) in the context of the ERA-NET MNT framework. Experimental measurements provided by IMT Bucharest

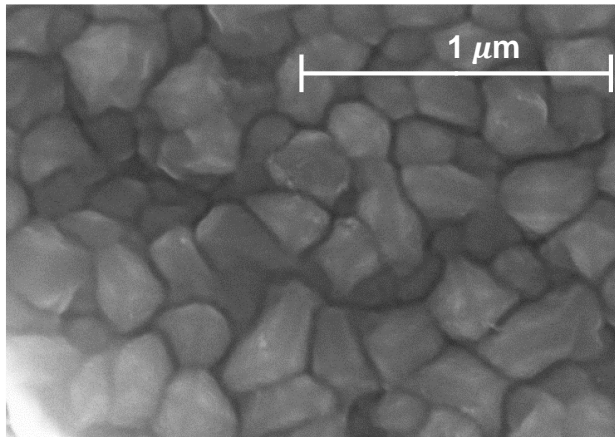
The problem

- MEMS structures
 - Are not several orders larger than their micro-structure size
 - Parameters-dependent manufacturing process
 - Low Pressure Chemical Vapor Deposition (LPCVD)
 - Properties depend on the temperature, time process, and flow gas conditions

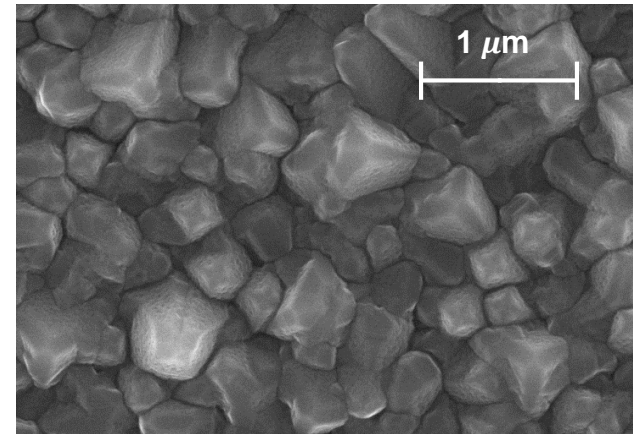


The problem

- Material structure: grain size distribution
 - Measurement of SEM (Scanning electron microscope)
 - Grain size dependent on the LPCVD temperature process
 - 2 μm -thick poly-silicon films



Deposition temperature: 580 °C



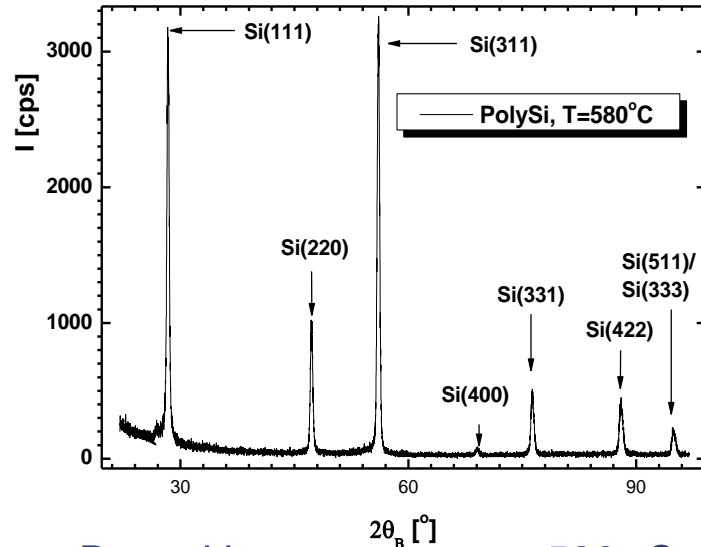
Deposition temperature: 650 °C

| Temperature [°C] | 580 | 610 | 630 | 650 |
|--|------|------|------|------|
| Average grain diameter [μm] | 0.21 | 0.45 | 0.72 | 0.83 |

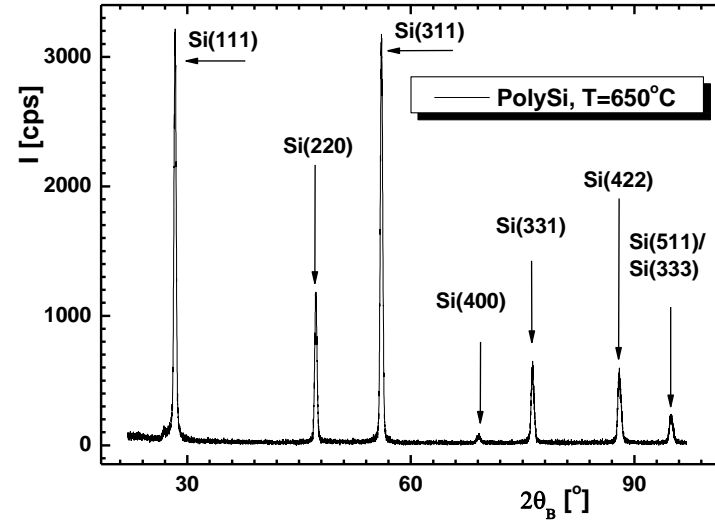
SEM images provided by IMT Bucharest, Rodica Voicu, Angela Baracu, Raluca Muller

The problem

- Material structure: grain orientation distribution
 - Grain orientation by XRD (X-ray Diffraction) measurements on 2 μm -thick poly-silicon films



Deposition temperature: 580 °C



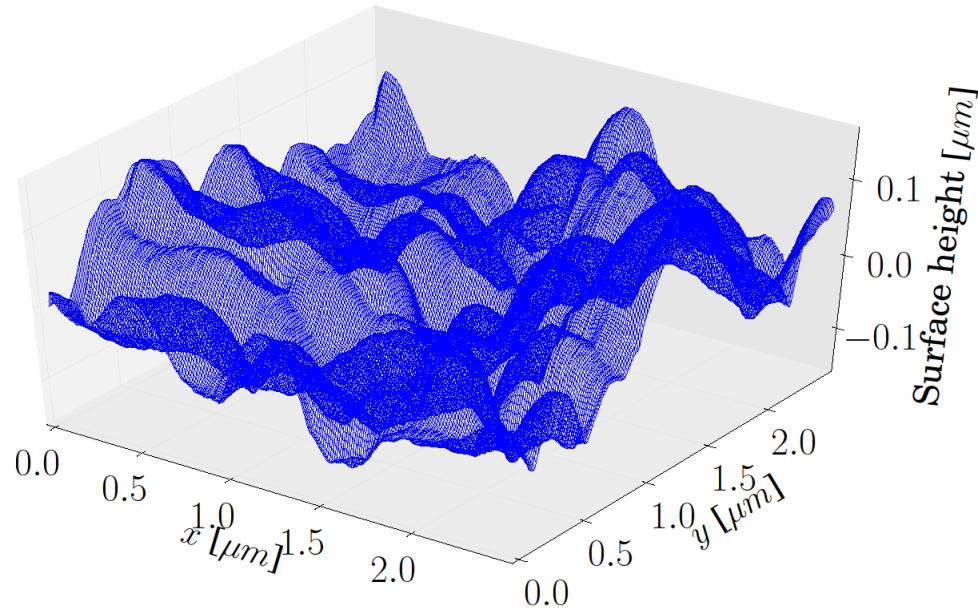
Deposition temperature: 630 °C

| Temperature [°C] | 580 | 610 | 630 | 650 |
|------------------|-------|-------|-------|-------|
| <111> [%] | 12.57 | 19.96 | 12.88 | 11.72 |
| <220> [%] | 7.19 | 13.67 | 7.96 | 7.59 |
| <311> [%] | 42.83 | 28.83 | 39.08 | 38.47 |
| <400> [%] | 4.28 | 5.54 | 3.13 | 3.93 |
| <331> [%] | 17.97 | 18.14 | 21.32 | 20.45 |
| <422> [%] | 15.15 | 13.86 | 15.63 | 17.84 |

XRD images provided by IMT Bucharest, Rodica Voicu, Angela Baracu, Raluca Muller

The problem

- Surface topology: asperity distribution
 - Upper surface topology by AFM (Atomic Force Microscope) measurements on 2 μm -thick poly-silicon films



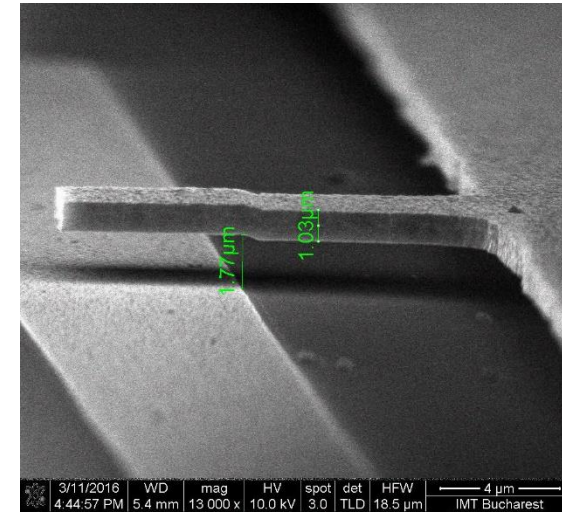
| | | | | |
|------------------------------------|------|------|------|------|
| Temperature [$^{\circ}\text{C}$] | 580 | 610 | 630 | 650 |
| Std deviation [nm] | 35.6 | 60.3 | 90.7 | 88.3 |

AFM data provided by IMT Bucharest, Rodica Voicu, Angela Baracu, Raluca Muller

The problem

- MEMS structures

- Are not several orders larger than their micro-structure size
- Parameters-dependent manufacturing process
 - Low Pressure Chemical Vapor Deposition (LPCVD)
 - Properties depend on the temperature, time process, and flow gas conditions
- As a result, their macroscopic properties can exhibit a **scatter**
 - Due to the fabrication process (photolithography, wet and dry etching)
 - Due to uncertainties of the material
 - ...

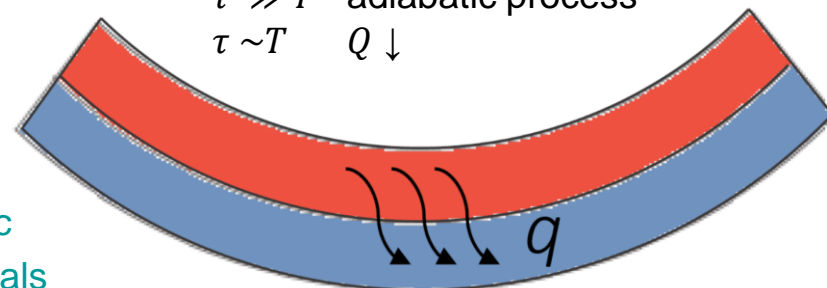


➔ The objective of this work is to estimate this scatter

- Application example

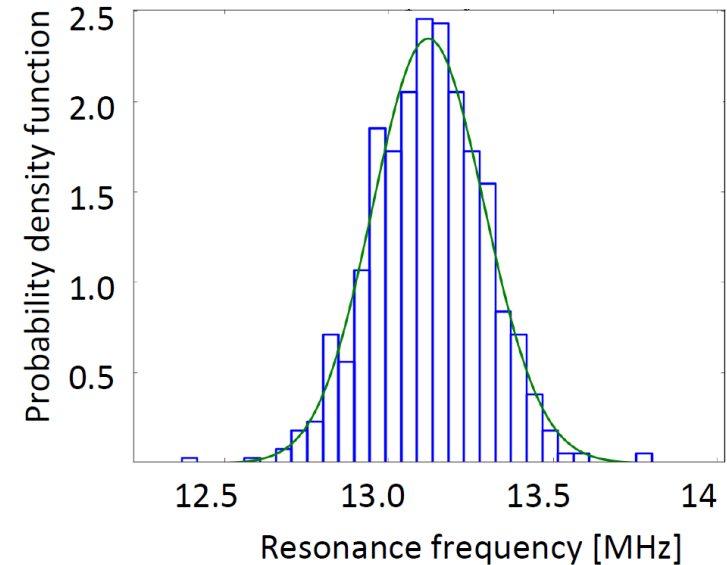
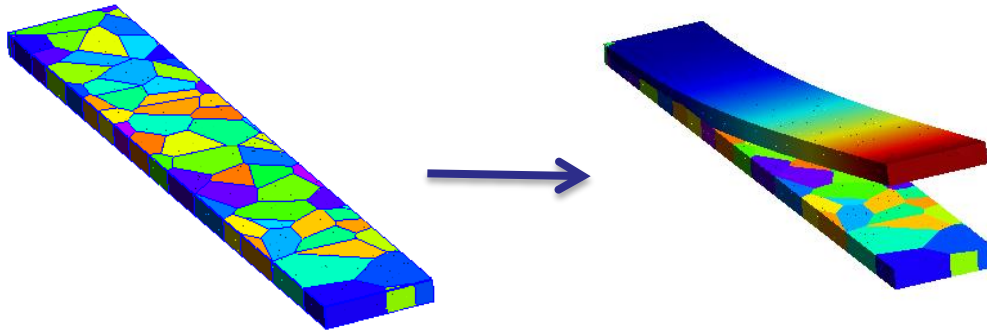
- Poly-silicon resonators
- Quantities of interest
 - Eigen frequency
 - Quality factor due to thermoelastic damping $Q \sim W/\Delta W$
 - Thermoelastic damping is a source of intrinsic material damping present in almost all materials

$\tau \ll T$ isothermal process
 $\tau \gg T$ adiabatic process
 $\tau \sim T$ $Q \downarrow$



Monte-Carlo for a fully modelled beam

- The first mode frequency distribution can be obtained with
 - A 3D beam with each grain modelled
 - Grains according to experimental measurements
 - Monte-Carlo simulations

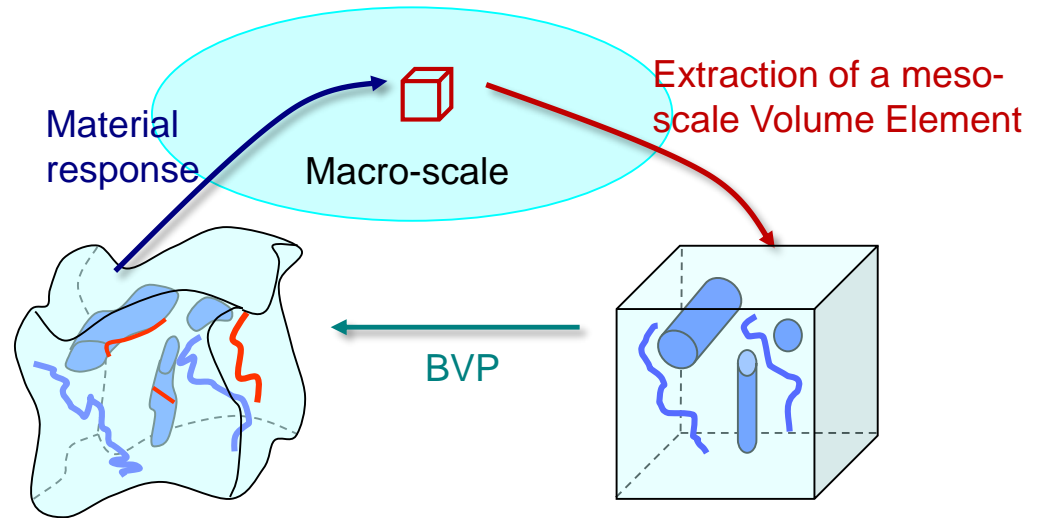


- Considering each grain is expensive and time consuming
 - ↳ Motivation for stochastic multi-scale methods

Motivations

- Multi-scale modelling

- 2 problems are solved concurrently
 - The macro-scale problem
 - The meso-scale problem (on a meso-scale Volume Element)



- Length-scales separation

$$L_{\text{macro}} \gg L_{\text{VE}} \gg L_{\text{micro}}$$

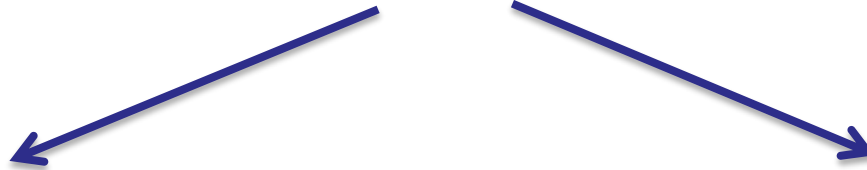
For accuracy: Size of the meso-scale volume element smaller than the characteristic length of the macro-scale loading

To be statistically representative: Size of the meso-scale volume element larger than the characteristic length of the micro-structure

Motivations

- For structures not several orders larger than the micro-structure size

$$L_{\text{macro}} \gg L_{\text{VE}} \sim L_{\text{micro}}$$



For accuracy: Size of the meso-scale volume element smaller than the characteristic length of the macro-scale loading

Meso-scale volume element no longer statistically representative: Stochastic Volume Elements*

- Possibility to propagate the uncertainties from the micro-scale to the macro-scale

*M Ostoja-Starzewski, X Wang, 1999

P Trovalusci, M Ostoja-Starzewski, M L De Bellis, A Murralli, 2015

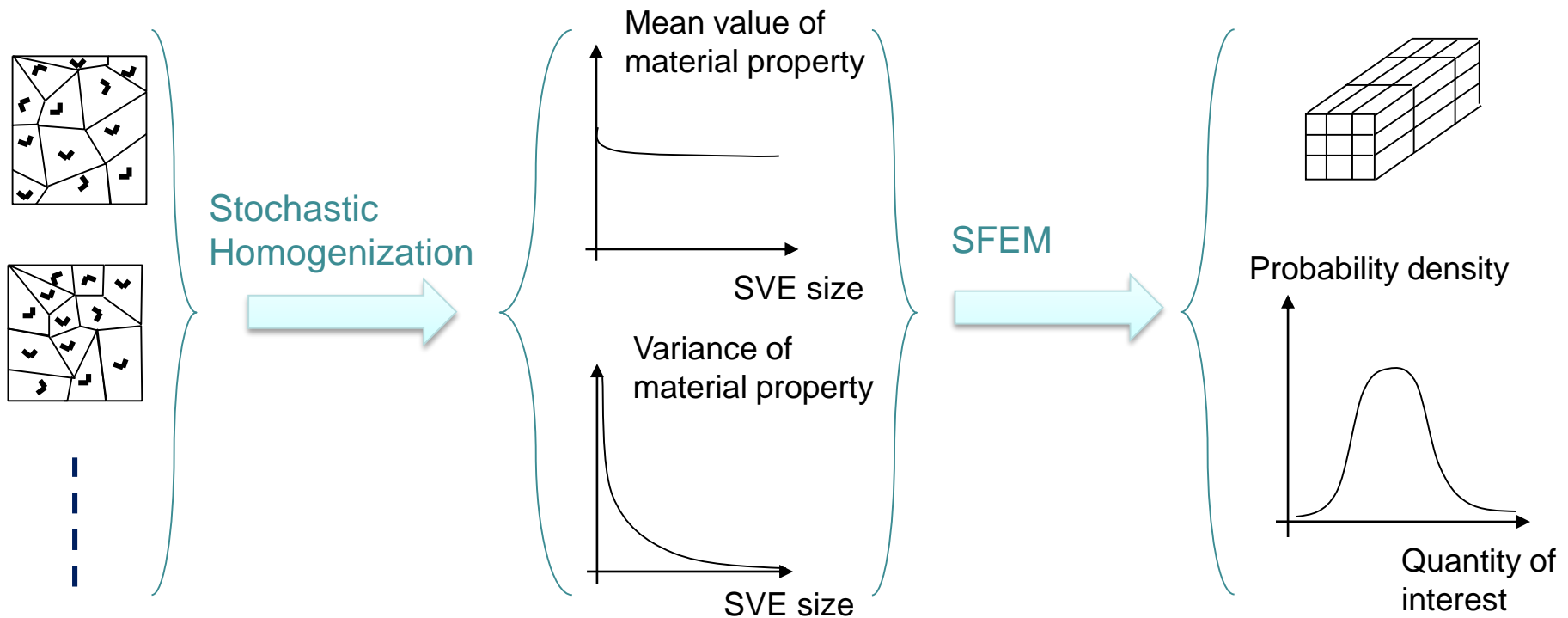
X. Yin, W. Chen, A. To, C. McVeigh, 2008

J. Guillemot, A. Noshadravan, C. Soize, R. Ghanem, 2011

....

A 3-scale process

| Grain-scale or micro-scale | Meso-scale | Macro-scale |
|--|---|---|
| <ul style="list-style-type: none"> ➤ Samples of the microstructure (volume elements) are generated ➤ Each grain has a random orientation | <ul style="list-style-type: none"> ➤ Intermediate scale ➤ The distribution of the material property $\mathbb{P}(C)$ is defined | <ul style="list-style-type: none"> ➤ Uncertainty quantification of the macro-scale quantity ➤ E.g. the first mode frequency $\mathbb{P}(f_1)$ /Quality factor $\mathbb{P}(Q)$ |



- **Thermo-mechanical problems**
 - Governing equations
 - Macro-scale stochastic finite element
 - Meso-scale volume elements
- **From the micro-scale to the meso-scale**
 - Thermo-mechanical homogenization
 - Definition of Stochastic Volume Elements (SVEs) & Stochastic homogenization
 - Need for a meso-scale random field
- **The meso-scale random field**
 - Definition of the thermo-mechanical meso-scale random field
 - Stochastic model of the random field: Spectral generator & non-Gaussian mapping
- **From the meso-scale to the macro-scale**
 - 3-Scale approach verification
 - Application to extract the quality factor
- **Extension to stochastic-plate finite elements**
 - Second-order stochastic homogenization
 - Rough Stochastic Volume Elements
 - Topology uncertainties effects

Thermo-mechanical problem

- Governing equations

- Thermo-mechanics

- Linear balance $\rho \ddot{\mathbf{u}} - \nabla \cdot \boldsymbol{\sigma} - \rho \mathbf{b} = 0$

- Clausius-Duhem inequality in terms of volume entropy rate $\dot{S} = -\frac{\nabla \cdot \mathbf{q}}{T}$

- Helmholtz free energy

$$\left\{ \begin{array}{l} \mathcal{F}(\boldsymbol{\varepsilon}, T) = \mathcal{F}_0(T) - \boldsymbol{\varepsilon} : \frac{\partial^2 \psi}{\partial \boldsymbol{\varepsilon} \partial \boldsymbol{\varepsilon}} : \boldsymbol{\alpha} (T - T_0) + \psi(\boldsymbol{\varepsilon}) \\ \boldsymbol{\sigma} = \left(\frac{\partial \mathcal{F}}{\partial \boldsymbol{\varepsilon}} \right)_T, \quad S = \left(\frac{\partial \mathcal{F}}{\partial T} \right)_\boldsymbol{\varepsilon} \quad \& \quad \left(\frac{\partial^2 \mathcal{F}_0}{\partial T \partial T} \right) = \rho C_v \end{array} \right.$$

- Strong form in terms of the displacements \mathbf{u} and temperature change ϑ (linear elasticity)

$$\hookrightarrow \left\{ \begin{array}{l} \rho \ddot{\mathbf{u}} - \nabla \cdot (\mathbb{C} : \dot{\boldsymbol{\varepsilon}} - \mathbb{C} : \boldsymbol{\alpha} \vartheta) - \rho \mathbf{b} = 0 \\ \rho C_v \dot{\vartheta} + T_0 \boldsymbol{\alpha} : \mathbb{C} : \dot{\boldsymbol{\varepsilon}} - \nabla \cdot (\boldsymbol{\kappa} \nabla \vartheta) = 0 \end{array} \right.$$

- Finite element discretization

$$\hookrightarrow \begin{bmatrix} \mathbf{M}(\rho) & \mathbf{0} \\ \mathbf{0} & \mathbf{0} \end{bmatrix} \begin{bmatrix} \ddot{\mathbf{u}} \\ \dot{\vartheta} \end{bmatrix} + \begin{bmatrix} \mathbf{0} & \mathbf{0} \\ \mathbf{D}_{\vartheta \mathbf{u}}(\boldsymbol{\alpha}, \mathbb{C}) & \mathbf{D}_{\vartheta \vartheta}(\rho C_v) \end{bmatrix} \begin{bmatrix} \dot{\mathbf{u}} \\ \dot{\vartheta} \end{bmatrix} + \begin{bmatrix} \mathbf{K}_{\mathbf{u}\mathbf{u}}(\mathbb{C}) & \mathbf{K}_{\mathbf{u}\vartheta}(\boldsymbol{\alpha}, \mathbb{C}) \\ \mathbf{0} & \mathbf{K}_{\vartheta\vartheta}(\boldsymbol{\kappa}) \end{bmatrix} \begin{bmatrix} \mathbf{u} \\ \vartheta \end{bmatrix} = \begin{bmatrix} \mathbf{F}_u \\ \mathbf{F}_\vartheta \end{bmatrix}$$

- Macro-scale stochastic finite element method
 - Meso-scale material properties subjected to uncertainties
 - Elasticity tensor $\mathbb{C}_M(\boldsymbol{\theta})$,
 - Heat conductivity tensor $\boldsymbol{\kappa}_M(\boldsymbol{\theta})$, and
 - Thermal expansion tensors $\boldsymbol{\alpha}_M(\boldsymbol{\theta})$
- in the sample space $\boldsymbol{\theta} \in \Omega$

$$\begin{bmatrix} \mathbf{M}(\rho_M) & \mathbf{0} \\ \mathbf{0} & \mathbf{0} \end{bmatrix} \begin{bmatrix} \ddot{\mathbf{u}} \\ \dot{\boldsymbol{\vartheta}} \end{bmatrix} + \begin{bmatrix} \mathbf{0} & \mathbf{0} \\ \mathbf{D}_{\vartheta u}(\boldsymbol{\alpha}_M, \mathbb{C}_M) & \mathbf{D}_{\vartheta\vartheta}(\rho_M c_{vM}) \end{bmatrix} \begin{bmatrix} \dot{\mathbf{u}} \\ \dot{\boldsymbol{\vartheta}} \end{bmatrix} + \begin{bmatrix} \mathbf{K}_{uu}(\mathbb{C}_M) & \mathbf{K}_{u\vartheta}(\boldsymbol{\alpha}_M, \mathbb{C}_M) \\ \mathbf{0} & \mathbf{K}_{\vartheta\vartheta}(\boldsymbol{\kappa}_M) \end{bmatrix} \begin{bmatrix} \mathbf{u} \\ \boldsymbol{\vartheta} \end{bmatrix} = \begin{bmatrix} \mathbf{F}_u \\ \mathbf{F}_\vartheta \end{bmatrix}$$

$$\hookrightarrow \begin{bmatrix} \mathbf{M} & \mathbf{0} \\ \mathbf{0} & \mathbf{0} \end{bmatrix} \begin{bmatrix} \ddot{\mathbf{u}} \\ \dot{\boldsymbol{\vartheta}} \end{bmatrix} + \begin{bmatrix} \mathbf{0} & \mathbf{0} \\ \mathbf{D}_{\vartheta u}(\boldsymbol{\theta}) & \mathbf{D}_{\vartheta\vartheta} \end{bmatrix} \begin{bmatrix} \dot{\mathbf{u}} \\ \dot{\boldsymbol{\vartheta}} \end{bmatrix} + \begin{bmatrix} \mathbf{K}_{uu}(\boldsymbol{\theta}) & \mathbf{K}_{u\vartheta}(\boldsymbol{\theta}) \\ \mathbf{0} & \mathbf{K}_{\vartheta\vartheta}(\boldsymbol{\theta}) \end{bmatrix} \begin{bmatrix} \mathbf{u} \\ \boldsymbol{\vartheta} \end{bmatrix} = \begin{bmatrix} \mathbf{F}_u \\ \mathbf{F}_\vartheta \end{bmatrix}$$

- Defining the random properties at the meso-scale by
 - Using micro-scale information (SEM, XRD, images)
 - Homogenization method

- Thermo-mechanical problems
 - Governing equations
 - Macro-scale stochastic finite element
 - Meso-scale volume elements
- **From the micro-scale to the meso-scale**
 - Thermo-mechanical homogenization
 - Definition of Stochastic Volume Elements (SVEs) & Stochastic homogenization
 - Need for a meso-scale random field
- The meso-scale random field
 - Definition of the thermo-mechanical meso-scale random field
 - Stochastic model of the random field: Spectral generator & non-Gaussian mapping
- From the meso-scale to the macro-scale
 - 3-Scale approach verification
 - Application to extract the quality factor
- Extension to stochastic-plate finite elements
 - Second-order stochastic homogenization
 - Rough Stochastic Volume Elements
 - Topology uncertainties effects

Thermo-mechanical problem

- Meso-scale Volume Elements (VE)

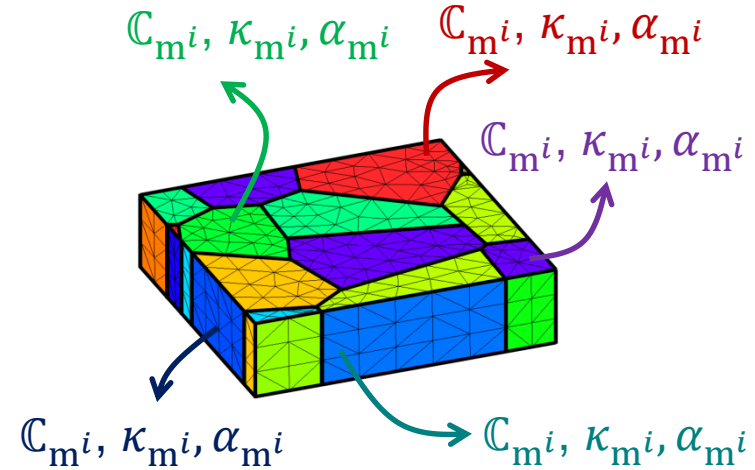
- Micro-scale material properties

- Elasticity tensor \mathbb{C}_m ,
- Heat conductivity tensor κ_m , and
- Thermal expansion tensors α_m

defined on each phase/heterogeneity

- Length scales separation assumptions

- VE small enough for the time for strain wave to propagate in the SVE to remain negligible
- VE small enough for the time variation of heat storage to remain negligible



$$\begin{bmatrix} \mathbf{M}(\rho_m) & \mathbf{0} \\ \mathbf{0} & \mathbf{0} \end{bmatrix} \begin{bmatrix} \ddot{\mathbf{u}} \\ \dot{\boldsymbol{\vartheta}} \end{bmatrix} + \begin{bmatrix} \mathbf{0} & \mathbf{0} \\ \mathbf{D}_{\vartheta u}(\alpha_m, \mathbb{C}_m) & \mathbf{D}_{\vartheta\vartheta}(\rho_m C_{vm}) \end{bmatrix} \begin{bmatrix} \dot{\mathbf{u}} \\ \dot{\boldsymbol{\vartheta}} \end{bmatrix} + \begin{bmatrix} \mathbf{K}_{uu}(\mathbb{C}_m) & \mathbf{K}_{u\vartheta}(\alpha_m, \mathbb{C}_m) \\ \mathbf{0} & \mathbf{K}_{\vartheta\vartheta}(\kappa_m) \end{bmatrix} \begin{bmatrix} \mathbf{u} \\ \boldsymbol{\vartheta} \end{bmatrix} = \begin{bmatrix} \mathbf{F}_u \\ \mathbf{F}_\vartheta \end{bmatrix}$$

$$\hookrightarrow \begin{bmatrix} \mathbf{K}_{uu} & \mathbf{K}_{u\vartheta} \\ \mathbf{0} & \mathbf{K}_{\vartheta\vartheta} \end{bmatrix} \begin{bmatrix} \mathbf{u} \\ \boldsymbol{\vartheta} \end{bmatrix} = \begin{bmatrix} \mathbf{F}_u \\ \mathbf{F}_\vartheta \end{bmatrix}$$

- Transition from meso-scale BVP realizations to the meso-scale random properties



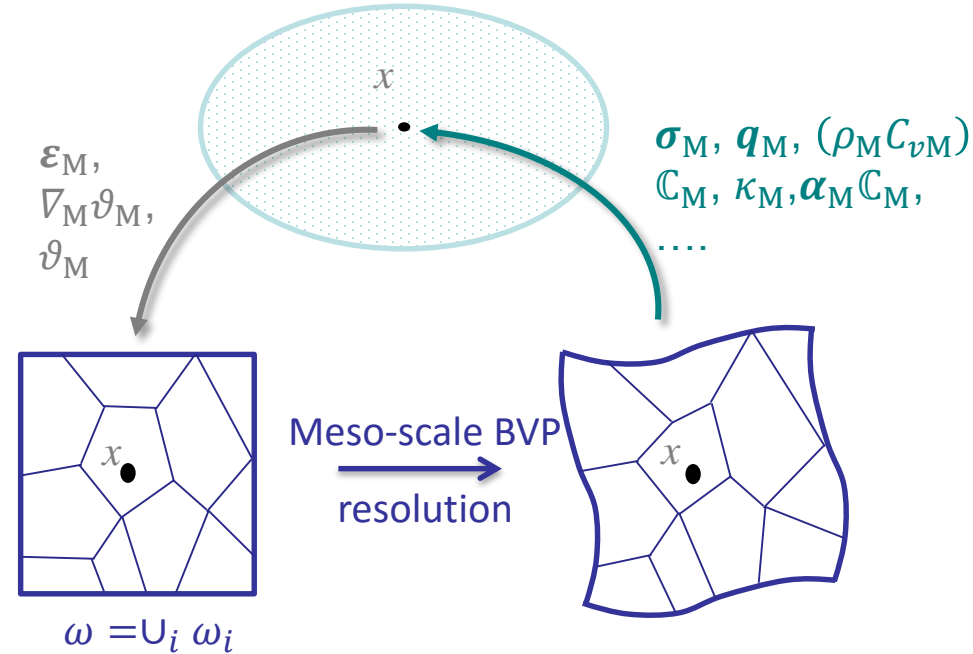
Stochastic thermo-mechanical homogenization

From the micro-scale to the meso-scale

- Thermo-mechanical homogenization

- Down-scaling

$$\left\{ \begin{array}{l} \varepsilon_M = \frac{1}{V(\omega)} \int_{\omega} \varepsilon_m d\omega \\ \nabla_M \vartheta_M = \frac{1}{V(\omega)} \int_{\omega} \nabla_m \vartheta_m d\omega \\ \vartheta_M = \frac{1}{V(\omega)} \int_{\omega} \frac{\rho_m c_{vm}}{\rho_M c_{vM}} \vartheta_m d\omega \end{array} \right.$$



- Meso-scale BVP fluctuation fields

$$\left\{ \begin{array}{l} \mathbf{u}_m = \varepsilon_M \cdot \mathbf{x} + \mathbf{u}' \\ \vartheta_m = \nabla_M \vartheta_M \cdot \mathbf{x} + \vartheta'_m \end{array} \right. \longrightarrow \left\{ \begin{array}{l} 0 = \int_{\partial\omega} \mathbf{u}' \otimes \mathbf{n} d\partial\omega \\ 0 = \int_{\partial\omega} \mathbf{n} \vartheta' d\partial\omega \end{array} \right.$$

→ Satisfied by periodic boundary conditions

- Thermo-mechanical homogenization (2)

- Upscaling

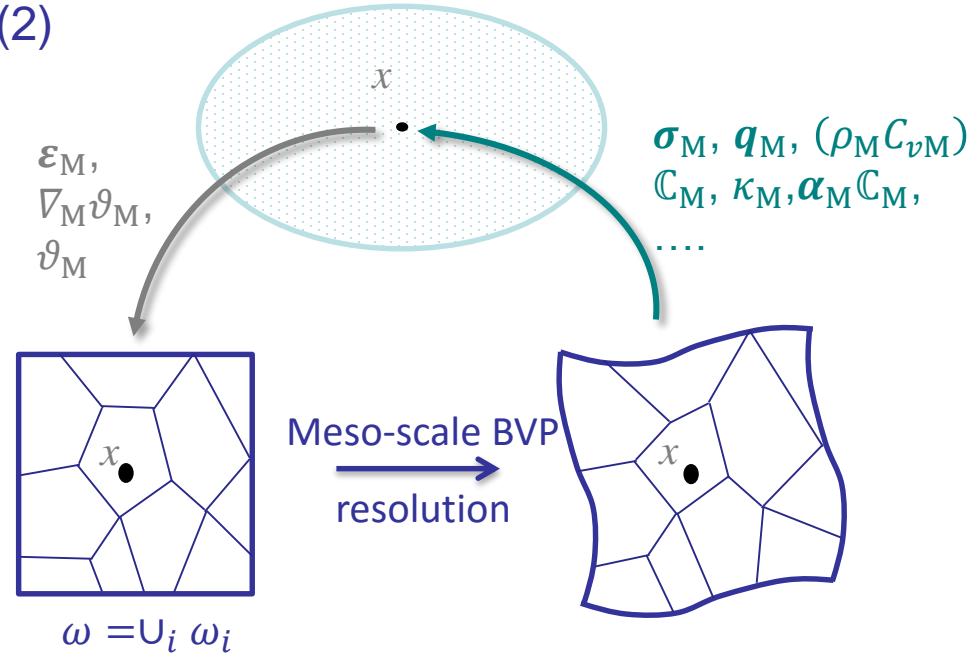
$$\left\{ \begin{aligned} \boldsymbol{\sigma}_M &= \frac{1}{V(\omega)} \int_{\omega} \boldsymbol{\sigma}_m d\omega \\ \mathbf{q}_M &= \frac{1}{V(\omega)} \int_{\omega} \mathbf{q}_m d\omega \\ \rho_M C_{vM} &= \frac{1}{V(\omega)} \int \rho_m C_{vm} dV \end{aligned} \right.$$

- Consistency

$$\left\{ \begin{aligned} \boldsymbol{\sigma}_M : \delta \boldsymbol{\varepsilon}_M &= \frac{1}{V(\omega)} \int_{\omega} \boldsymbol{\sigma}_m : \delta \boldsymbol{\varepsilon}_m d\omega \\ \frac{\mathbf{q}_M \cdot \nabla_M \delta \vartheta_M}{T_M} &\simeq \frac{1}{T_M V(\omega)} \int_{\omega} \mathbf{q}_m \cdot \nabla_m \delta \vartheta_m d\omega \\ \rho_M C_{vM} \vartheta_M &= \frac{1}{V(\omega)} \int_{\omega} \rho_m C_{vm} \vartheta_m d\omega \end{aligned} \right. \longrightarrow \left\{ \begin{aligned} 0 &= \int_{\partial \omega} (\boldsymbol{\sigma}_m \cdot \mathbf{n}) \cdot \mathbf{u}' d\omega \\ 0 &= \int_{\partial \omega} (\mathbf{q}_m \cdot \mathbf{n}) \vartheta' d\omega \\ \vartheta_M &= \frac{1}{V(\omega)} \int_{\omega} \frac{\rho_m C_{vm}}{\rho_M C_{vM}} \vartheta_m d\omega \end{aligned} \right.$$



Satisfied by periodic boundary conditions & volume constraint

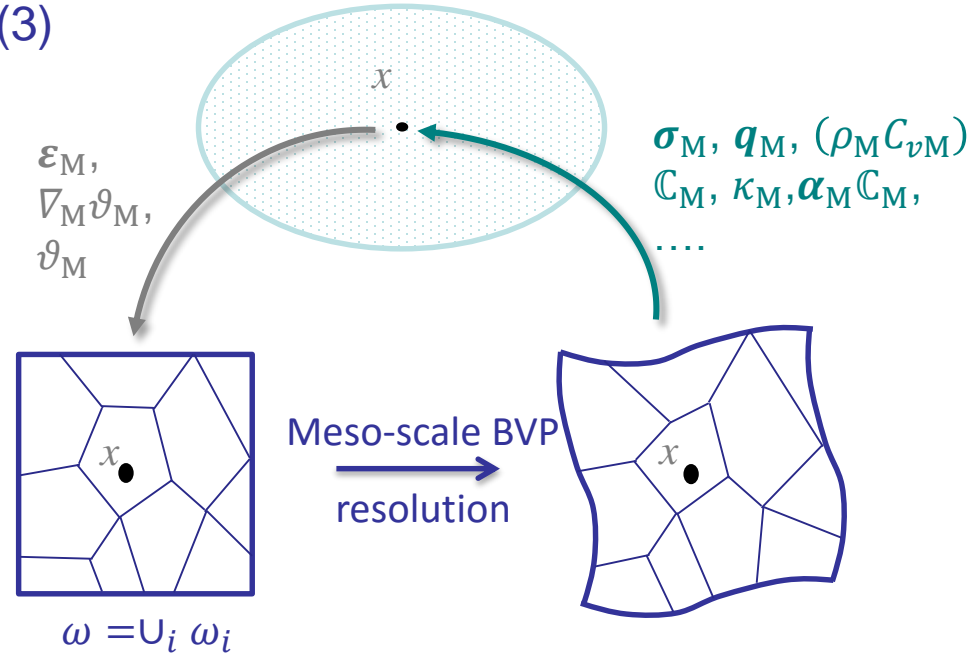


From the micro-scale to the meso-scale

- Thermo-mechanical homogenization (3)

- Micro-scale BVP

$$\left\{ \begin{array}{l} \begin{bmatrix} \mathbf{K}_{uu} & \mathbf{K}_{u\vartheta} \\ \mathbf{0} & \mathbf{K}_{\vartheta\vartheta} \end{bmatrix} \begin{bmatrix} \mathbf{u} \\ \vartheta \end{bmatrix} = \begin{bmatrix} \mathbf{F}_u \\ \mathbf{F}_\vartheta \end{bmatrix} \\ \mathbf{C} \begin{bmatrix} \mathbf{u} \\ \vartheta \end{bmatrix} = \mathbf{S} \begin{bmatrix} \nabla_M \mathbf{u}_M \\ \nabla_M \vartheta_M \\ \vartheta_M \end{bmatrix} \end{array} \right.$$



- Solution is the stationary point of

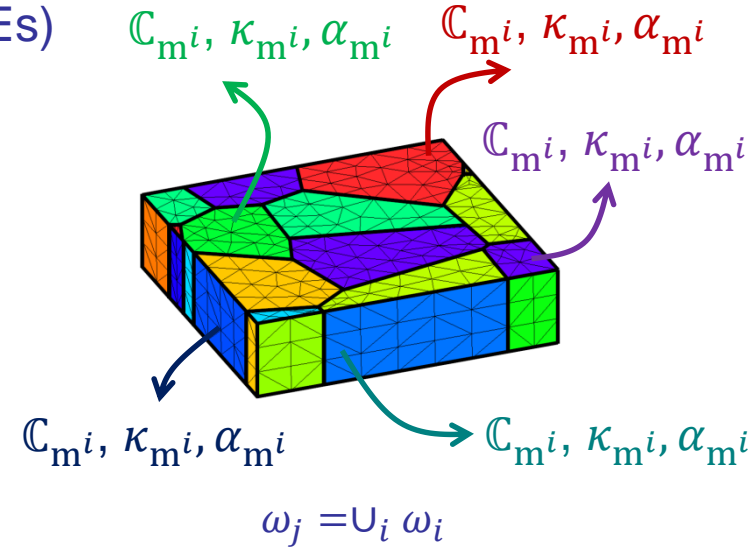
$$\Psi = \begin{bmatrix} \mathbf{u} \\ \vartheta \end{bmatrix}^T \begin{bmatrix} \mathbf{K}_{uu} & \mathbf{K}_{u\vartheta} \\ \mathbf{0} & \mathbf{K}_{\vartheta\vartheta} \end{bmatrix} \begin{bmatrix} \mathbf{u} \\ \vartheta \end{bmatrix} - \lambda^T \left[\mathbf{C} \begin{bmatrix} \mathbf{u} \\ \vartheta \end{bmatrix} - \mathbf{S} \begin{bmatrix} \nabla_M \mathbf{u}_M \\ \nabla_M \vartheta_M \\ \vartheta_M \end{bmatrix} \right]$$

$$\left\{ \begin{array}{l} \sigma_M = \frac{1}{V(\omega)} \frac{\partial \Psi}{\partial \mathbf{u}_M \otimes \nabla_M} \\ q_M = \frac{1}{V(\omega)} \frac{\partial \Psi}{\partial \nabla_M \vartheta_M} \end{array} \right. \longrightarrow \left\{ \begin{array}{l} \mathbb{C}_M = \frac{\partial \sigma_M}{\partial \mathbf{u}_M \otimes \nabla_M} \quad \& \quad \alpha_M: \mathbb{C}_M = - \frac{\partial \sigma_M}{\partial \vartheta_M} \\ \kappa_M = - \frac{\partial q_M}{\partial \nabla_M \vartheta_M} \end{array} \right.$$

From the micro-scale to the meso-scale

- Definition of Stochastic Volume Elements (SVEs)

- Poisson Voronoï tessellation realizations
 - SVE realization ω_j
- Each grain ω_i is assigned material properties
 - $\mathbb{C}_{m^i}, \kappa_{m^i}, \alpha_{m^i}$,
 - Defined from silicon crystal properties
- Each \mathbb{C}_{m^i} is assigned a random orientation
 - Following XRD distributions



- Stochastic homogenization

- Several SVE realizations
- For each SVE $\omega_j = \cup_i \omega_i$

$$\mathbb{C}_{m^i}, \kappa_{m^i}, \alpha_{m^i} \quad \forall i$$



Computational
homogenization

$$\mathbb{C}_{Mj}, \kappa_{Mj}, \alpha_{Mj}$$

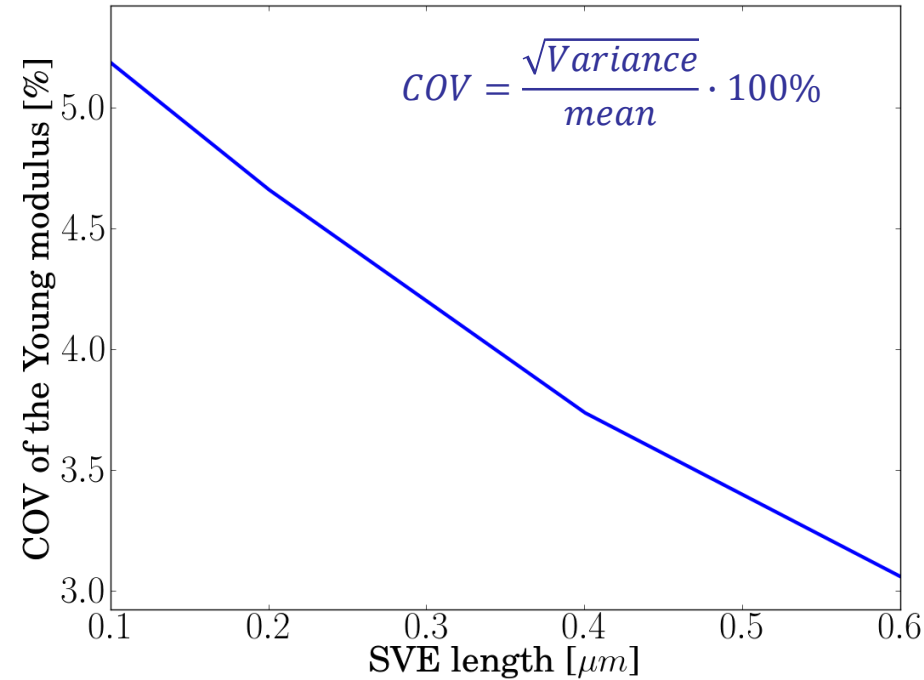
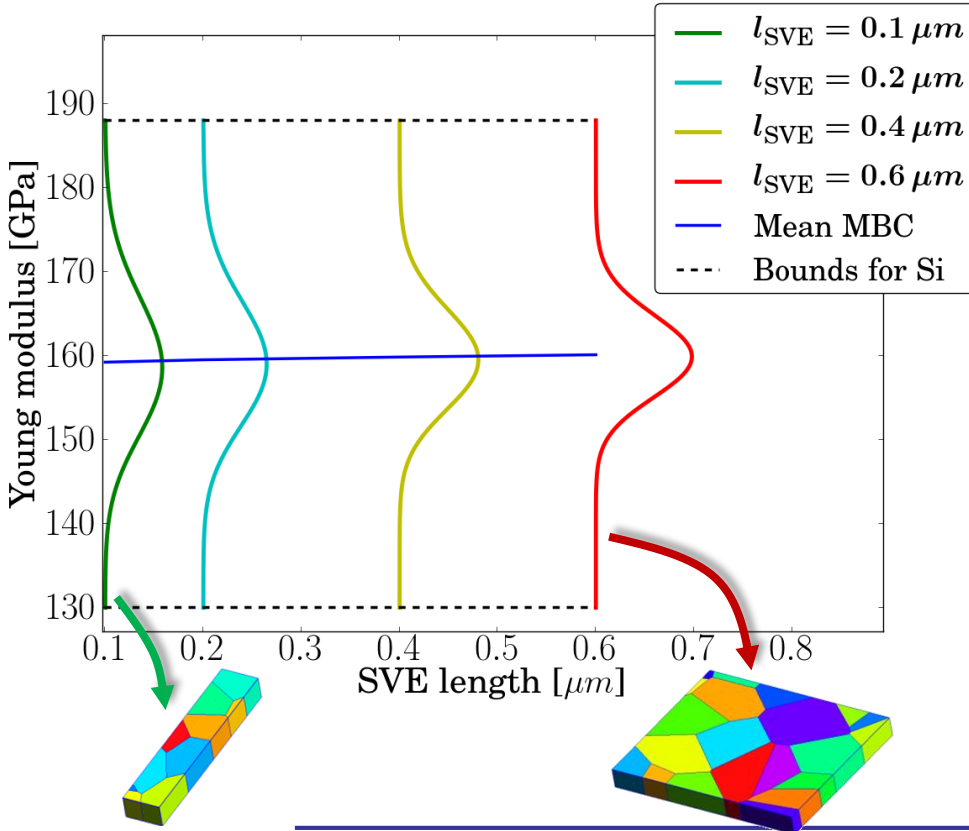
Samples of the meso-scale
homogenized
elasticity tensors

- Homogenized material tensors not unique as statistical representativeness is lost*

*C. Huet, 1990

From the micro-scale to the meso-scale

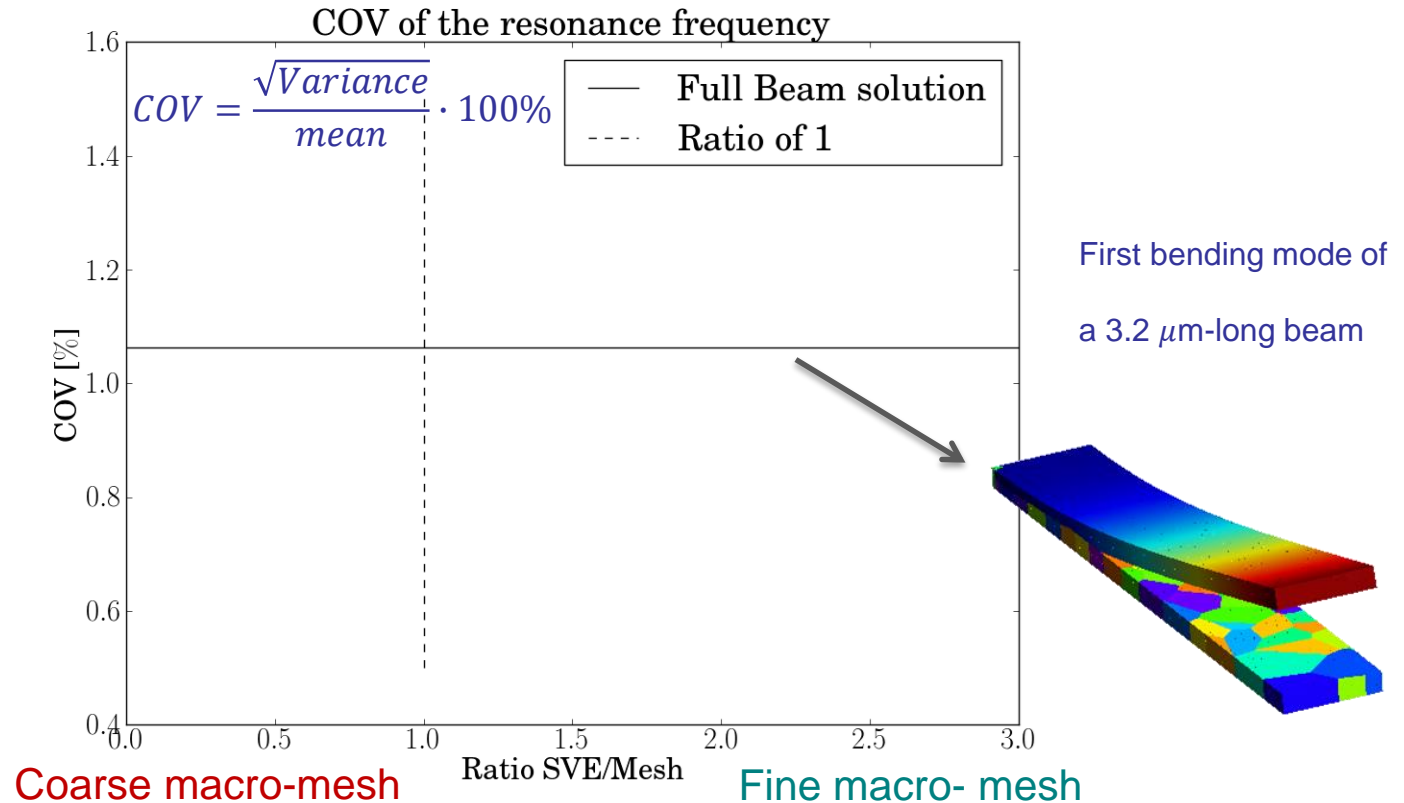
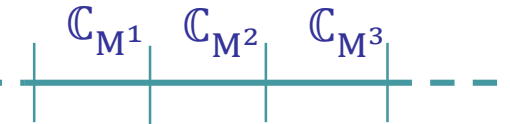
- Distribution of the apparent meso-scale elasticity tensor \mathbb{C}_M
 - For large SVEs, the apparent tensor tends to the effective (and unique) one



- The bounds do not depend on the SVE size but on the silicon elasticity tensor
- However, the larger the SVE, the lower the probability to be close to the bounds

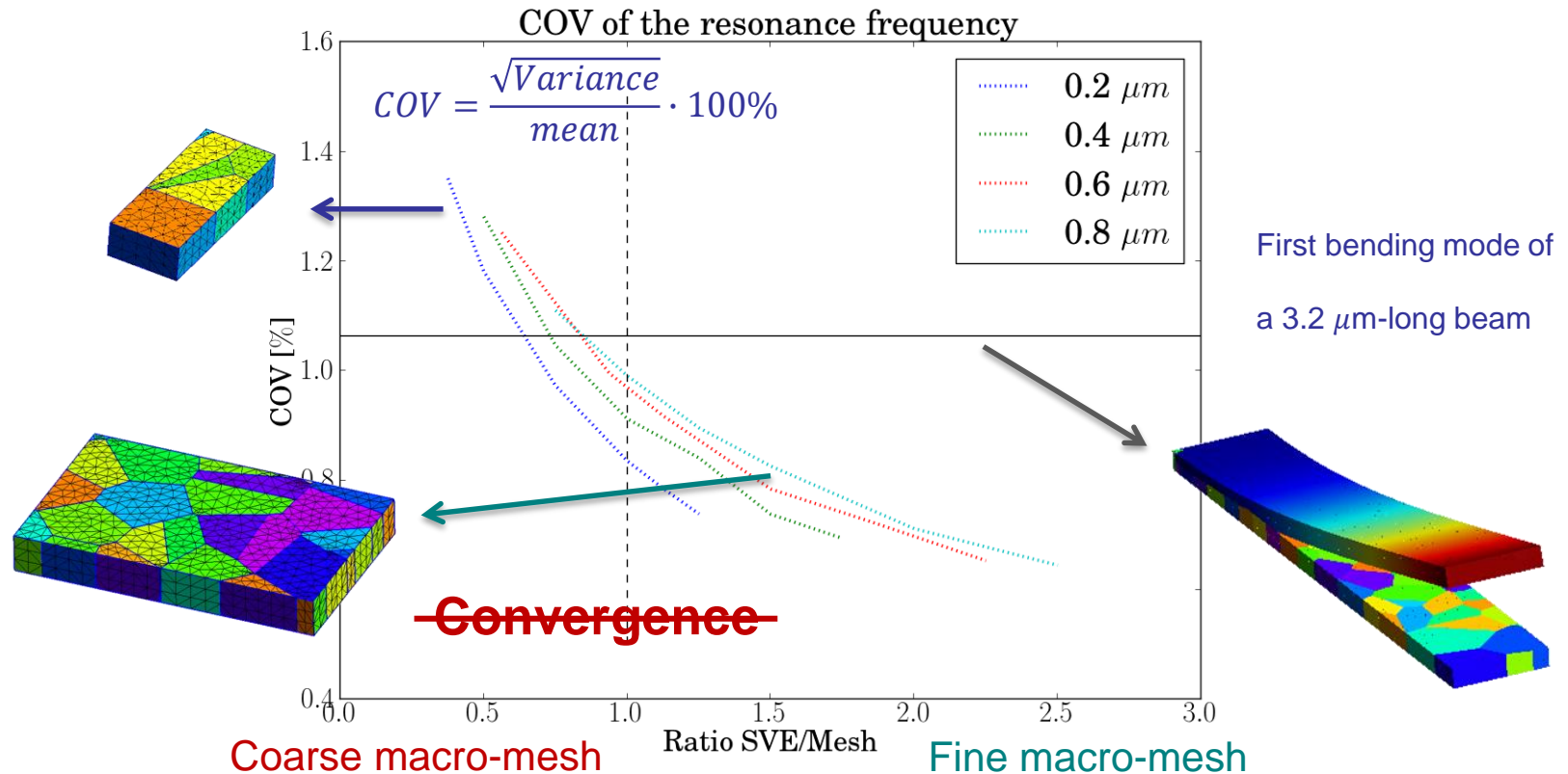
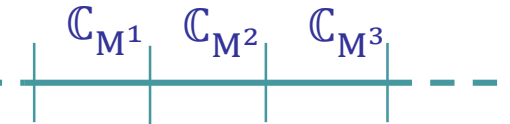
From the micro-scale to the meso-scale

- Use of the meso-scale distribution with macro-scale finite elements
 - Beam macro-scale finite elements
 - Use of the meso-scale distribution as a random variable
 - Monte-Carlo simulations



From the micro-scale to the meso-scale

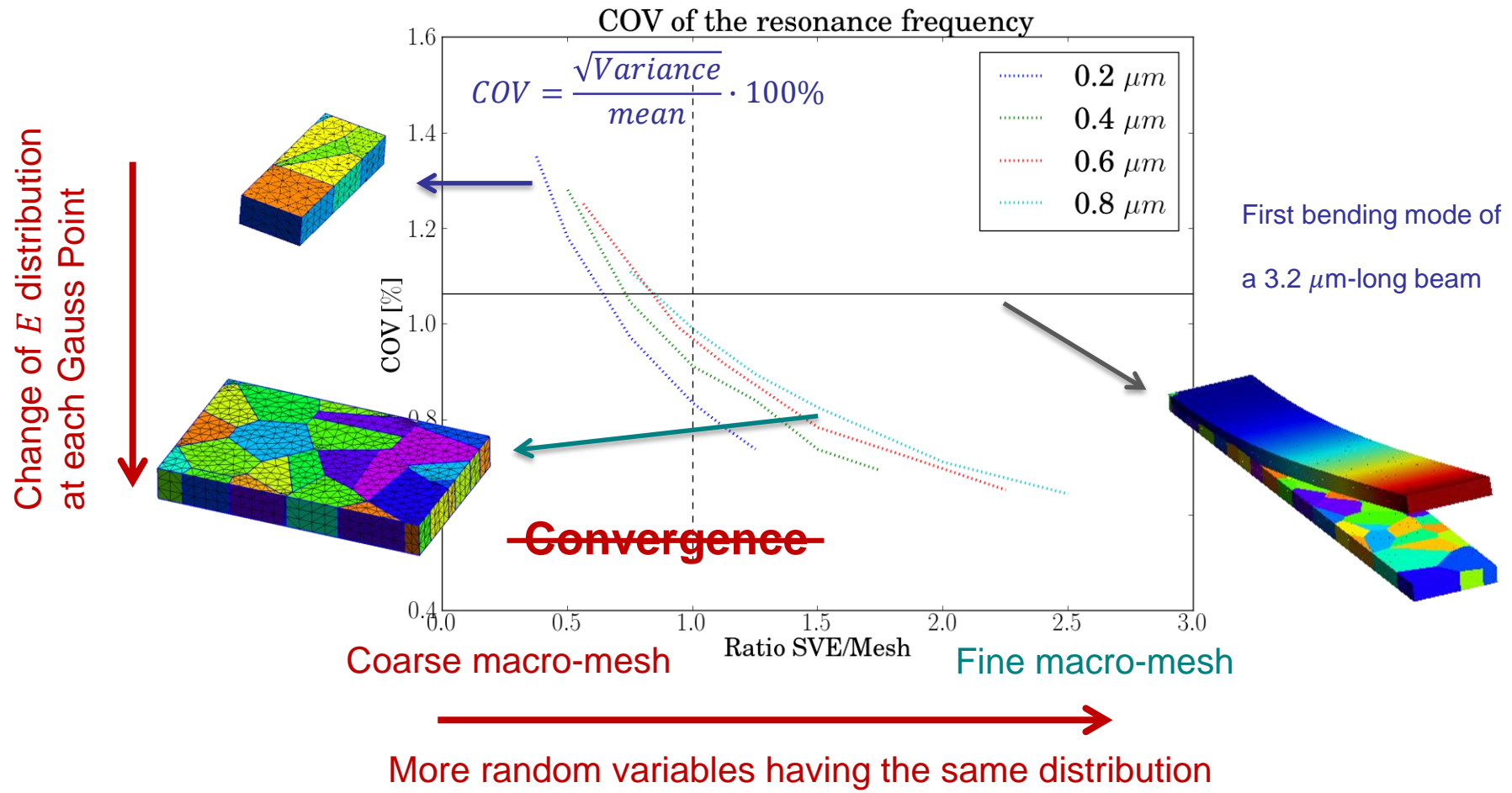
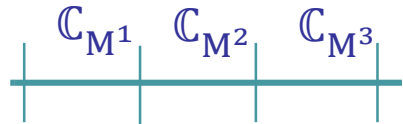
- Use of the meso-scale distribution with macro-scale finite elements
 - Beam macro-scale finite elements
 - Use of the meso-scale distribution as a random variable
 - Monte-Carlo simulations



- No convergence: the macro-scale distribution (first resonance frequency) depends on SVE and mesh sizes

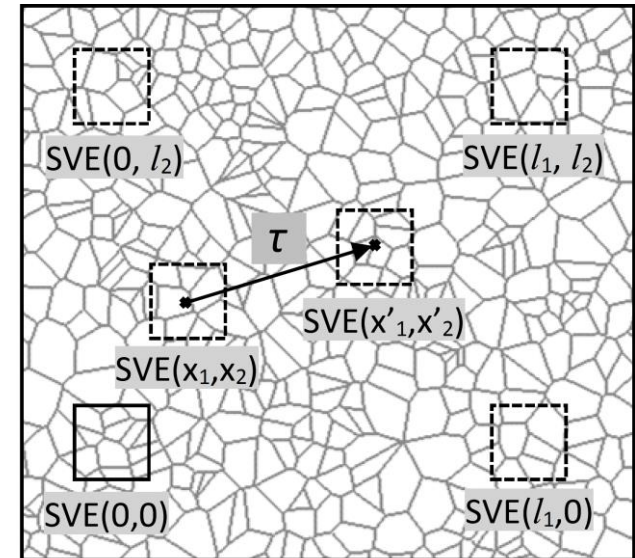
From the micro-scale to the meso-scale

- Use of the meso-scale distribution with macro-scale finite elements
 - Beam macro-scale finite elements
 - Use of the meso-scale distribution as a random variable
 - Monte-Carlo simulations



From the micro-scale to the meso-scale

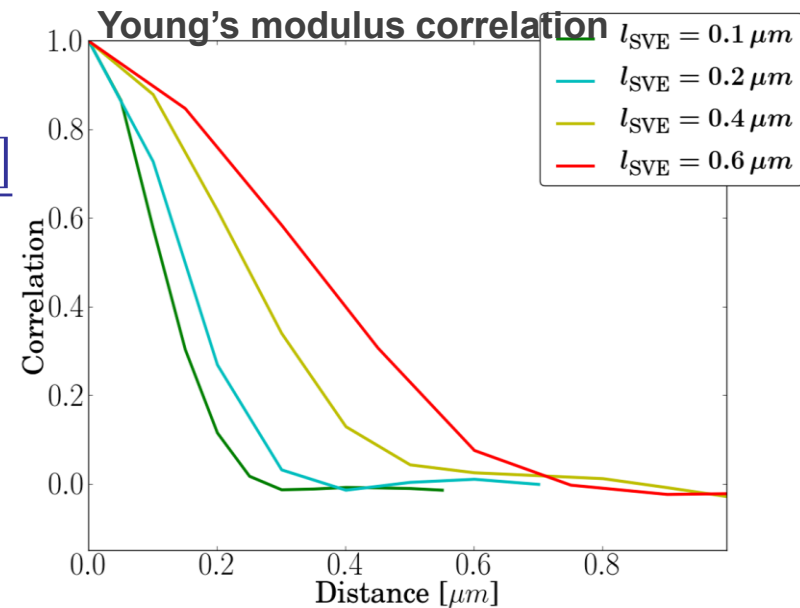
- Need for a meso-scale random field
 - Introduction of the (meso-scale) spatial correlation
 - Define large tessellations
 - SVEs extracted at different distances in each tessellation
 - Evaluate the spatial correlation between the components of the meso-scale material operators
 - For example, in 1D-elasticity
 - Young's modulus correlation



$$R_{E_x}(\tau) = \frac{\mathbb{E}[(\mathbf{E}_x(x) - \mathbb{E}(\mathbf{E}_x))(\mathbf{E}_x(x + \tau) - \mathbb{E}(\mathbf{E}_x))]}{\mathbb{E}[(\mathbf{E}_x - \mathbb{E}(\mathbf{E}_x))^2]}$$

- Correlation length

$$L_{E_x} = \frac{\int_{-\infty}^{\infty} R_{E_x}(\tau) d\tau}{R_{E_x}(0)}$$



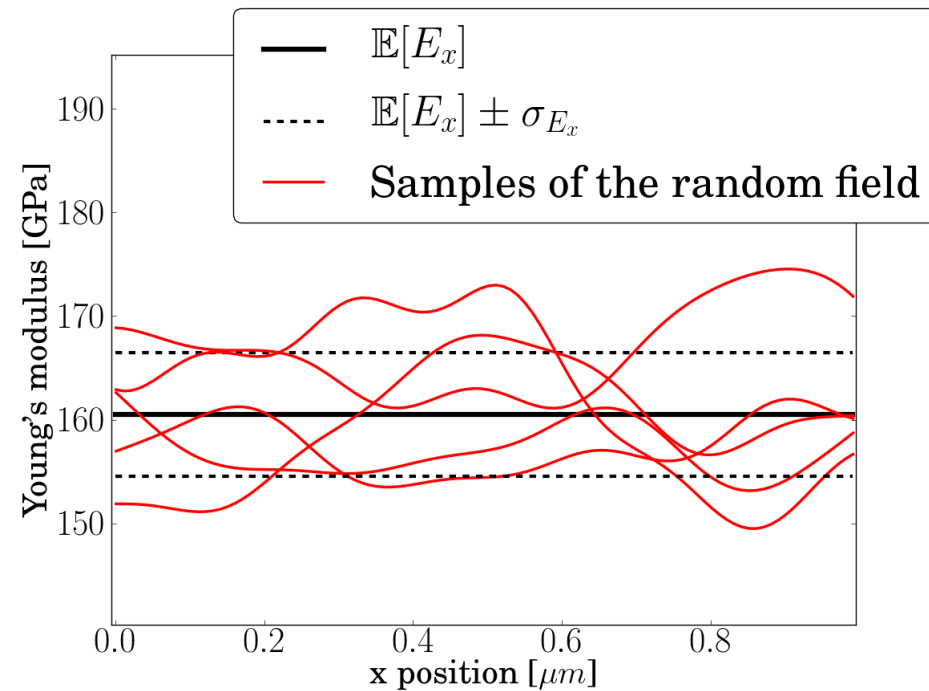
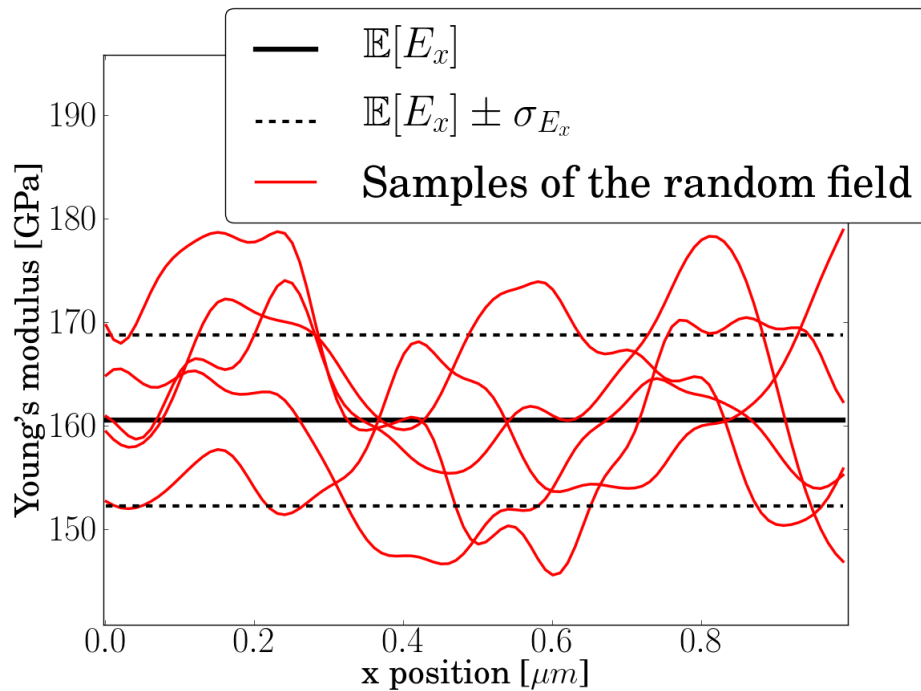
From the micro-scale to the meso-scale

- Need for a meso-scale random field (2)
 - The meso-scale random field is characterized by the correlation length L_{E_x}
 - The correlation length L_{E_x} depends on the SVE size

Random field with different SVEs sizes

$l_{\text{SVE}} = 0.1 \mu\text{m}$

$l_{\text{SVE}} = 0.4 \mu\text{m}$



From the micro-scale to the meso-scale

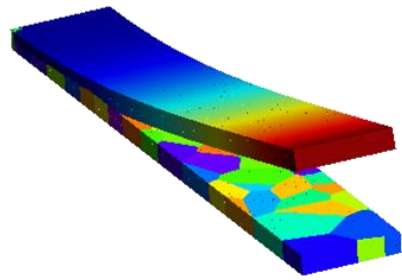
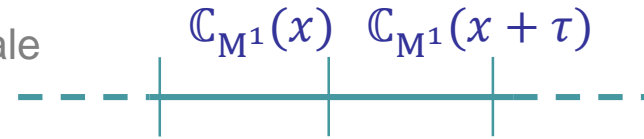
- Need for a meso-scale random field (3)

- Use of the meso-scale random field

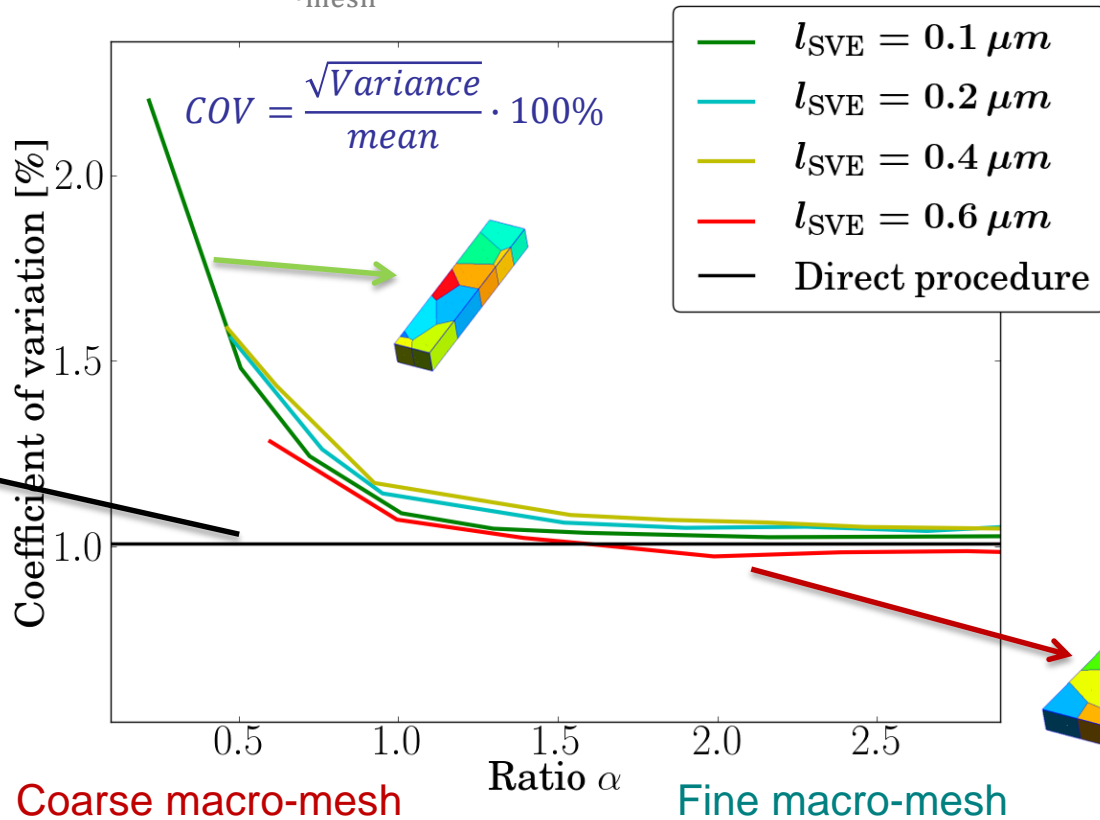
- Monte-Carlo simulations at the macro-scale

- Macro-scale beam elements of size l_{mesh}

- Convergence in terms of $\alpha = \frac{L_{Ex}}{l_{\text{mesh}}}$

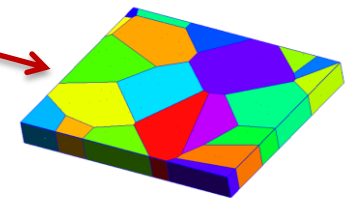


First bending mode of a $3.2 \mu\text{m}$ -long beam



Coarse macro-mesh

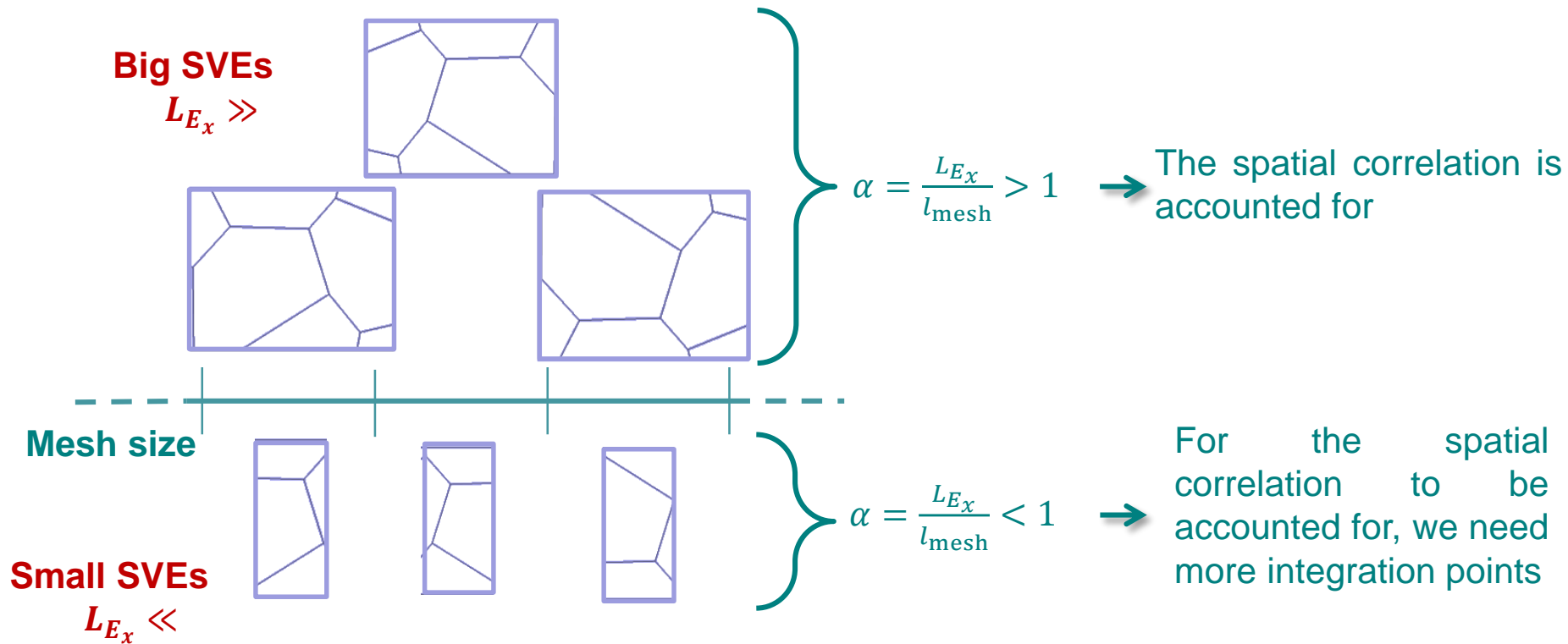
Fine macro-mesh



From the micro-scale to the meso-scale

- Need for a meso-scale random field (3)

- Effect of the ratio $\alpha = \frac{L_{Ex}}{l_{mesh}}$ (Only one gauss point in one element)



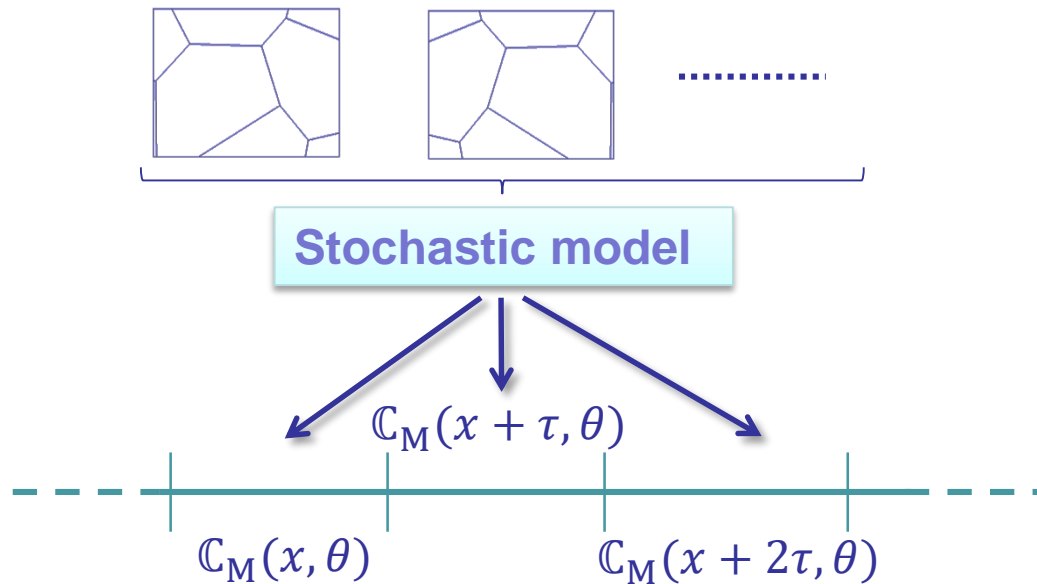
- For extreme values of α :
 - $\alpha \gg 1$: no more scale separation if $l_{SVE} \sim L_{macro}$
 - $\alpha \ll 1$: loss of microstructural details if $l_{SVE} \sim L_{micro}$

- Thermo-mechanical problems
 - Governing equations
 - Macro-scale stochastic finite element
 - Meso-scale volume elements
- From the micro-scale to the meso-scale
 - Thermo-mechanical homogenization
 - Definition of Stochastic Volume Elements (SVEs) & Stochastic homogenization
 - Need for a meso-scale random field
- **The meso-scale random field**
 - Definition of the thermo-mechanical meso-scale random field
 - Stochastic model of the random field: Spectral generator & non-Gaussian mapping
- From the meso-scale to the macro-scale
 - 3-Scale approach verification
 - Application to extract the quality factor
- Extension to stochastic-plate finite elements
 - Second-order stochastic homogenization
 - Rough Stochastic Volume Elements
 - Topology uncertainties effects

The meso-scale random field

- Use of the meso-scale distribution with stochastic (macro-scale) finite elements
 - Use of the meso-scale random field
 - Monte-Carlo simulations at the macro-scale
 - BUT we do not want to evaluate the random field from the stochastic homogenization for each simulation → Meso-scale random field from a generator

Stochastic model of meso-scale
elasticity tensors



- Definition of the thermo-mechanical meso-scale random field

- Elasticity tensor $\mathbb{C}_M(x, \theta)$ (matrix form \mathbf{C}_M) & thermal conductivity κ_M are bounded
 - Ensure existence of their inverse
 - Define lower bounds \mathbb{C}_L and κ_L such that

$$\left\{ \begin{array}{ll} \boldsymbol{\varepsilon} : (\mathbb{C}_M - \mathbb{C}_L) : \boldsymbol{\varepsilon} > 0 & \forall \boldsymbol{\varepsilon} \\ \nabla \vartheta \cdot (\boldsymbol{\kappa}_M - \boldsymbol{\kappa}_L) \cdot \nabla \vartheta > 0 & \forall \nabla \vartheta \end{array} \right.$$

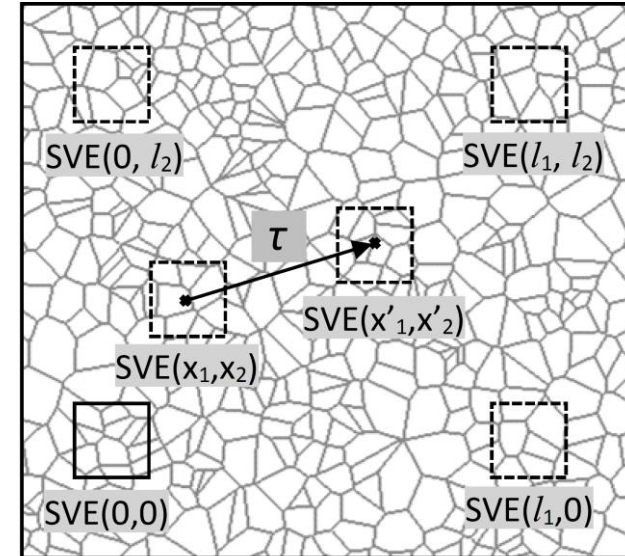
- Use a Cholesky decomposition when semi-definite tensors are required

$$\left\{ \begin{array}{l} \mathbf{C}_M(x, \theta) = \mathbf{C}_L + (\bar{\mathbf{A}} + \mathcal{A}'(x, \theta))^T (\bar{\mathbf{A}} + \mathcal{A}'(x, \theta)) \\ \boldsymbol{\kappa}_M(x, \theta) = \boldsymbol{\kappa}_L + (\bar{\mathbf{B}} + \mathcal{B}'(x, \theta))^T (\bar{\mathbf{B}} + \mathcal{B}'(x, \theta)) \\ \alpha_{M,ij}(x, \theta) = \bar{\nu}^{(t)} + \boldsymbol{\nu}'^{(t)}(x, \theta) \end{array} \right.$$

- We define the homogenous zero-mean random field $\boldsymbol{\nu}'(x, \theta)$, with as entries
 - Elasticity tensor $\mathcal{A}'(x, \theta) \Rightarrow \boldsymbol{\nu}'^{(1)} \dots \boldsymbol{\nu}'^{(21)}$,
 - Heat conductivity tensor $\mathcal{B}'(x, \theta) \Rightarrow \boldsymbol{\nu}'^{(22)} \dots \boldsymbol{\nu}'^{(27)}$
 - Thermal expansion tensors $\boldsymbol{\nu}'^{(t)} \Rightarrow \boldsymbol{\nu}'^{(28)} \dots \boldsymbol{\nu}'^{(33)}$

The meso-scale random field

- Characterization of the meso-scale random field
 - Generate large tessellation realizations
 - For each tessellation realization
 - Extract SVEs centred on $\mathbf{x} + \boldsymbol{\tau}$
 - For each SVE evaluate $\mathbb{C}_M(\mathbf{x} + \boldsymbol{\tau}), \kappa_M(\mathbf{x} + \boldsymbol{\tau}), \alpha_M(\mathbf{x} + \boldsymbol{\tau})$
 - From the set of realizations $\mathbb{C}_M(\mathbf{x}, \boldsymbol{\theta}), \kappa_M(\mathbf{x}, \boldsymbol{\theta}), \alpha_M(\mathbf{x}, \boldsymbol{\theta})$
 - Evaluate the bounds \mathbb{C}_L and κ_L
 - Apply the Cholesky decomposition $\Rightarrow \mathcal{A}'(\mathbf{x}, \boldsymbol{\theta}), \mathcal{B}'(\mathbf{x}, \boldsymbol{\theta})$
 - Fill the 33 entries of the zero-mean homogenous field $\boldsymbol{\nu}'(\mathbf{x}, \boldsymbol{\theta})$
 - NB: for the thermal conductivity we use a grain-size dependent empirical relation
 - Compute the auto-/cross-correlation matrix



$$R_{\boldsymbol{\nu}'}^{(rs)}(\boldsymbol{\tau}) = \frac{\mathbb{E} \left[\left(\boldsymbol{\nu}'^{(r)}(\mathbf{x}) - \mathbb{E}(\boldsymbol{\nu}'^{(r)}) \right) \left(\boldsymbol{\nu}'^{(s)}(\mathbf{x} + \boldsymbol{\tau}) - \mathbb{E}(\boldsymbol{\nu}'^{(s)}) \right) \right]}{\sqrt{\mathbb{E} \left[\left(\boldsymbol{\nu}'^{(r)} - \mathbb{E}(\boldsymbol{\nu}'^{(r)}) \right)^2 \right] \mathbb{E} \left[\left(\boldsymbol{\nu}'^{(s)} - \mathbb{E}(\boldsymbol{\nu}'^{(s)}) \right)^2 \right]}}$$

The meso-scale random field

- Stochastic model of the meso-scale random field: Spectral generator*

- Start from the auto-/cross-covariance matrix

$$\tilde{R}_{\mathbf{v}'}^{(rs)}(\boldsymbol{\tau}) = \sigma_{\mathbf{v}'(r)} \sigma_{\mathbf{v}'(s)} R_{\mathbf{v}'}^{(rs)}(\boldsymbol{\tau}) = \mathbb{E} \left[\left(\mathbf{v}'^{(r)}(\mathbf{x}) - \mathbb{E}(\mathbf{v}'^{(r)}) \right) \left(\mathbf{v}'^{(s)}(\mathbf{x} + \boldsymbol{\tau}) - \mathbb{E}(\mathbf{v}'^{(s)}) \right) \right]$$

- Evaluate the spectral density matrix from the periodized zero-padded matrix $\tilde{R}_{\mathbf{v}'}^P(\boldsymbol{\tau})$

$$\mathbf{S}_{\mathbf{v}'}^{(rs)}[\boldsymbol{\omega}^{(m)}] = \sum_n \tilde{R}_{\mathbf{v}'}^P{}^{(rs)}[\boldsymbol{\tau}^{(n)}] e^{-2\pi i \boldsymbol{\tau}^{(n)} \cdot \boldsymbol{\omega}^{(m)}} \quad \& \quad \mathbf{S}_{\mathbf{v}'}[\boldsymbol{\omega}^{(m)}] = \mathbf{H}_{\mathbf{v}'}[\boldsymbol{\omega}^{(m)}] \mathbf{H}_{\mathbf{v}'}^*[\boldsymbol{\omega}^{(m)}]$$

- $\boldsymbol{\omega}$ gathers the discrete frequencies
- $\boldsymbol{\tau}$ gathers the discrete spatial locations

- Generate a Gaussian random field $\mathbf{v}'(\mathbf{x}, \boldsymbol{\theta})$

$$\mathbf{v}'^{(r)}(\mathbf{x}, \boldsymbol{\theta}) = \sqrt{2\Delta\omega} \Re \left(\sum_s \sum_m \mathbf{H}_{\mathbf{v}'}^{(rs)}[\boldsymbol{\omega}^{(m)}] \eta^{(s,m)} e^{2\pi i (\mathbf{x} \cdot \boldsymbol{\omega}^{(m)} + \boldsymbol{\theta}^{(s,m)})} \right)$$

- $\boldsymbol{\eta}$ and $\boldsymbol{\theta}$ are independent random variables

- Quid if a non-Gaussian distribution is sought?

*Shinozuka, M., Deodatis, G., 1988

The meso-scale random field

- Stochastic model of the meso-scale random field: non-Gaussian mapping*

- Start from micro-sampling of the stochastic homogenization

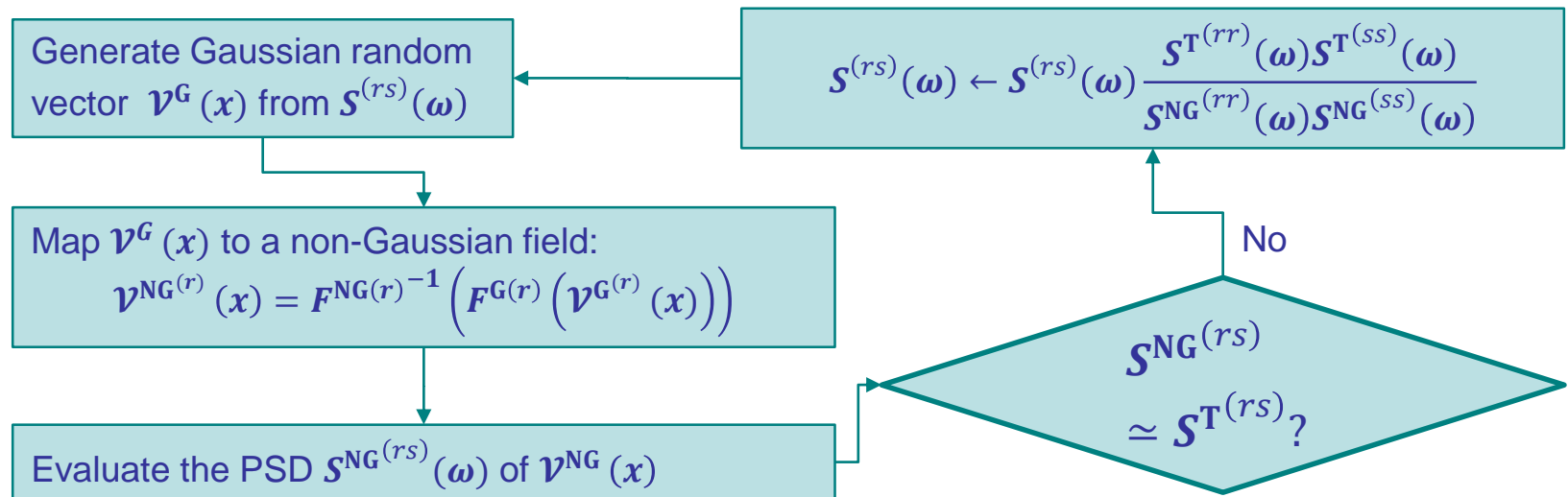
- The continuous form of the targeted PSD function

$$S^{T(rs)}(\omega) = \Delta\tau S_{\mathcal{V}'}^{(rs)}[\omega^{(m)}] = \Delta\tau \sum_n \tilde{R}_{\mathcal{V}'}^{P(rs)}[\tau^{(n)}] e^{-2\pi i \tau^{(n)} \cdot \omega^{(m)}}$$

- The targeted marginal distribution density function $F^{NG(r)}$ of the random variable $\mathcal{V}'^{(r)}$

- A marginal Gaussian distribution $F^{G(r)}$ of zero-mean and targeted variance $\sigma_{\mathcal{V}'^{(r)}}$

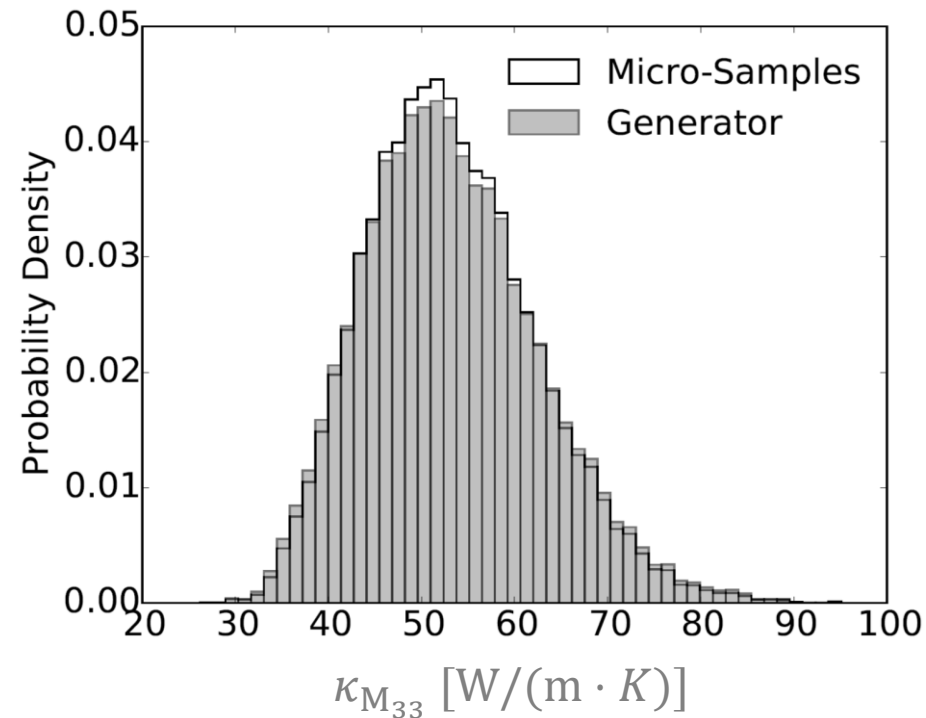
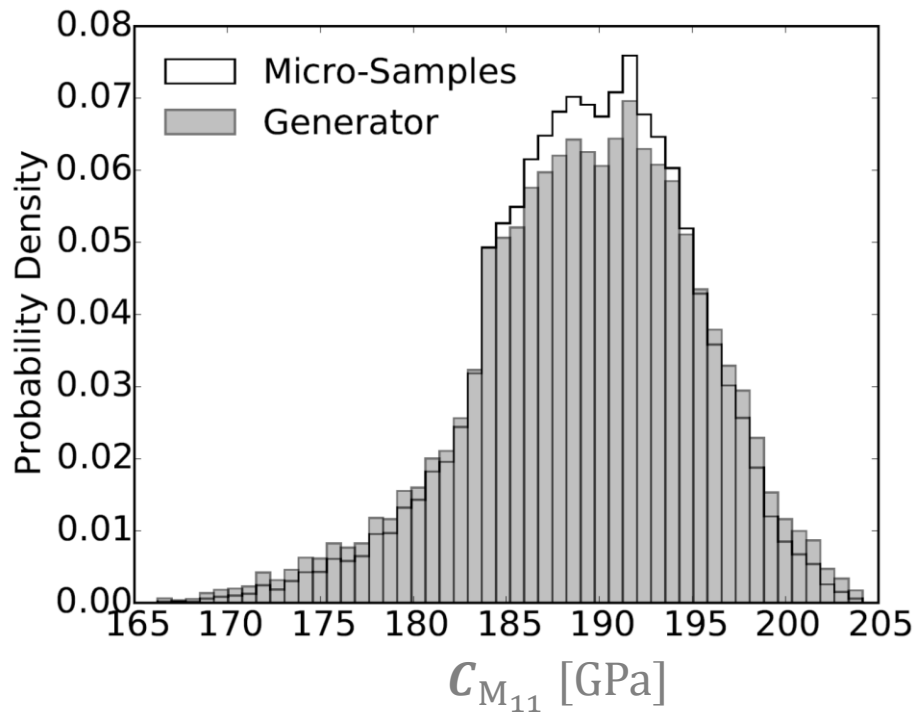
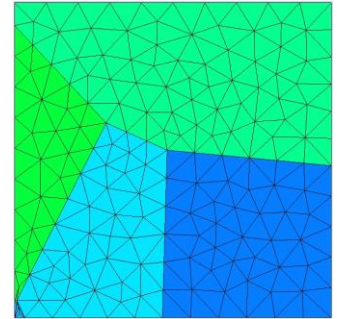
- Iterate



*Deodatis, G., Micaletti, R., 2001

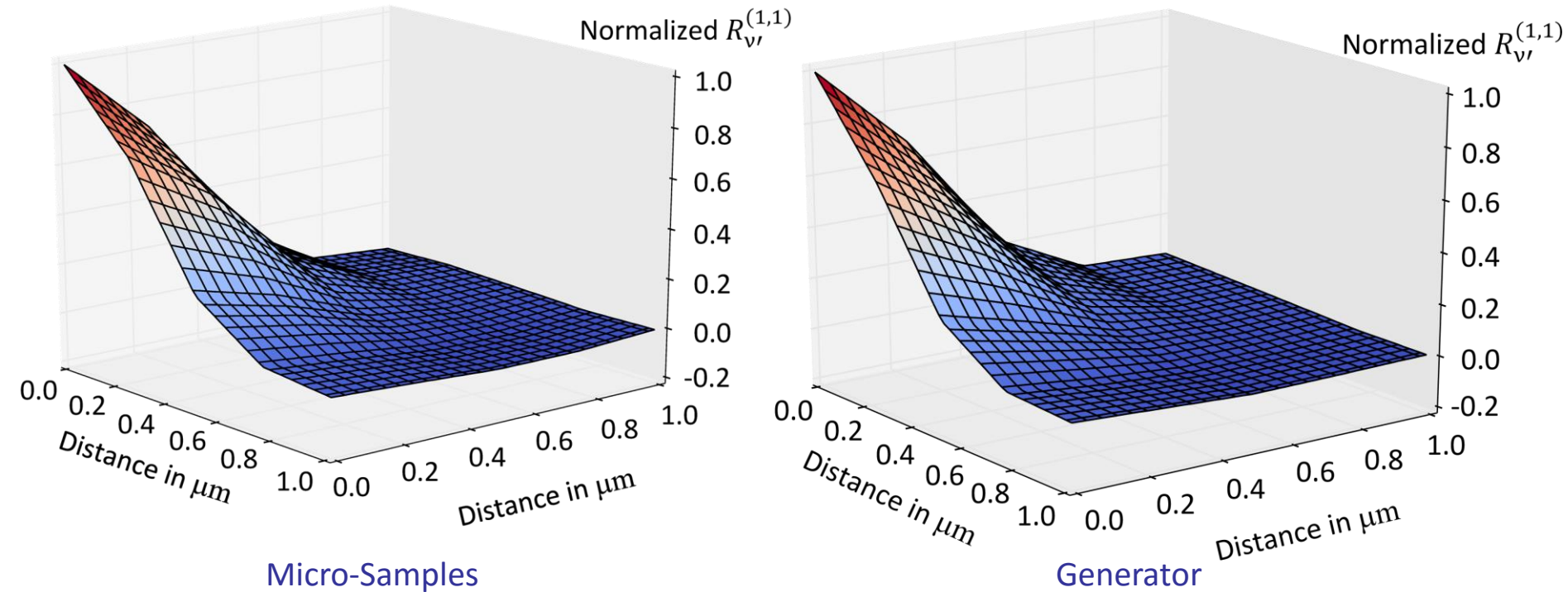
The meso-scale random field

- Polysilicon film deposited at 610 °C
 - SVE size of $0.5 \times 0.5 \mu\text{m}^2$
 - Comparison between micro-samples and generated field PDF



The meso-scale random field

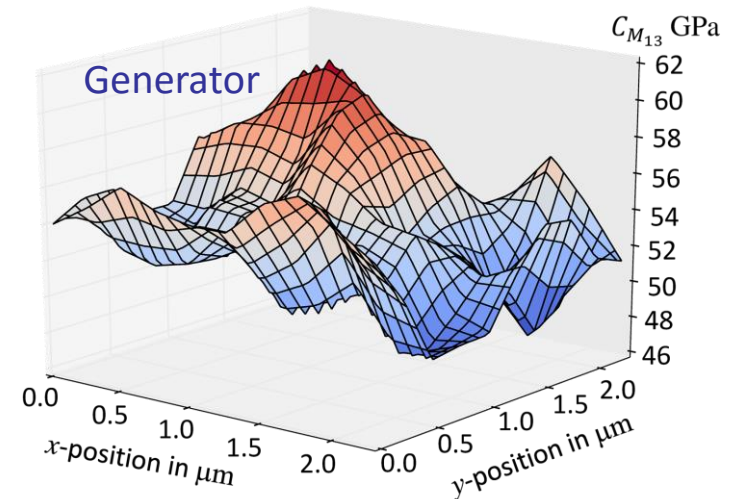
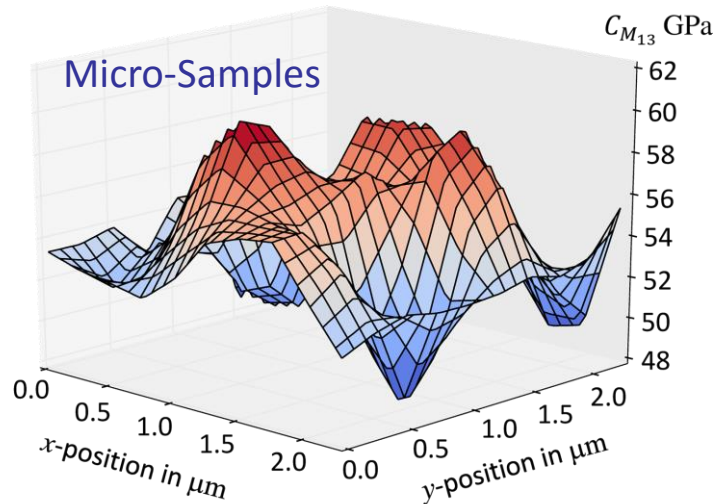
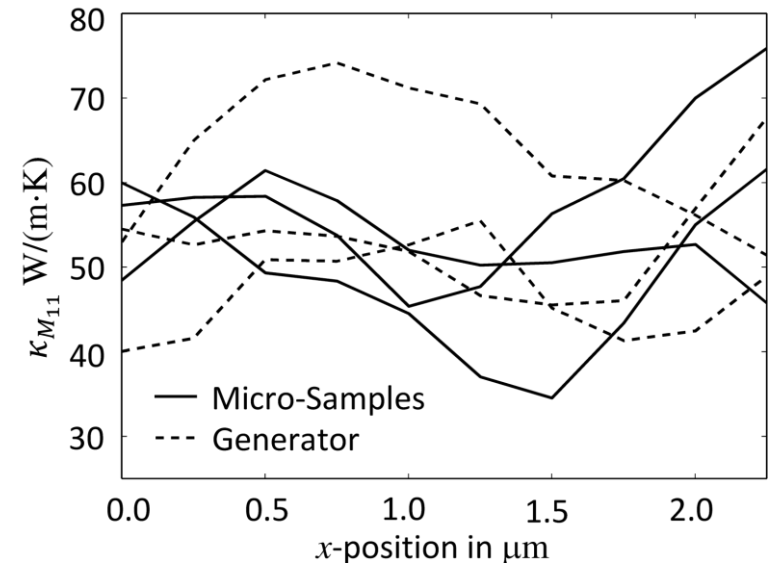
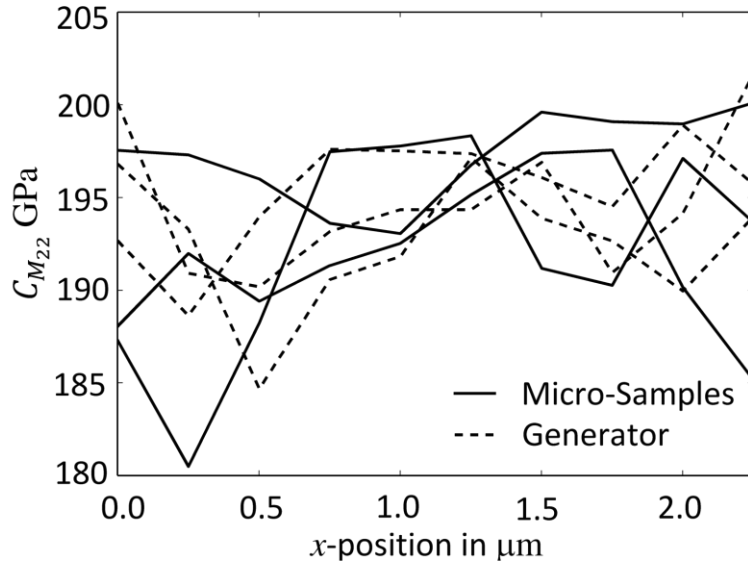
- Polysilicon film deposited at 610 °C (2)
 - Comparison between micro-samples and generated field cross-correlations



The meso-scale random field

- Polysilicon film deposited at 610 °C (3)

- Comparison between micro-samples and generated random field realizations



- Thermo-mechanical problems
 - Governing equations
 - Macro-scale stochastic finite element
 - Meso-scale volume elements
- From the micro-scale to the meso-scale
 - Thermo-mechanical homogenization
 - Definition of Stochastic Volume Elements (SVEs) & Stochastic homogenization
 - Need for a meso-scale random field
- The meso-scale random field
 - Definition of the thermo-mechanical meso-scale random field
 - Stochastic model of the random field: Spectral generator & non-Gaussian mapping
- **From the meso-scale to the macro-scale**
 - 3-Scale approach verification
 - Application to extract the quality factor
- Extension to stochastic-plate finite elements
 - Second-order stochastic homogenization
 - Rough Stochastic Volume Elements
 - Topology uncertainties effects

From the meso-scale to the macro-scale

- 3-Scale approach verification with direct Monte-Carlo simulations

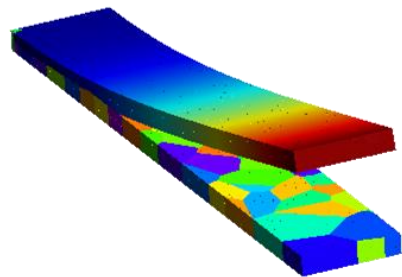
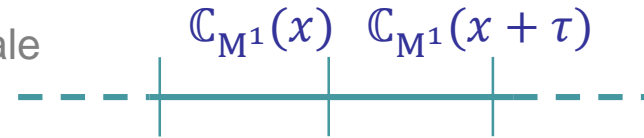
- Use of the meso-scale random field



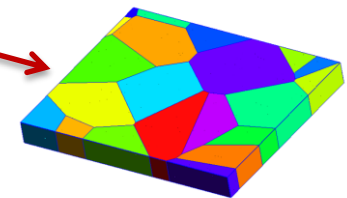
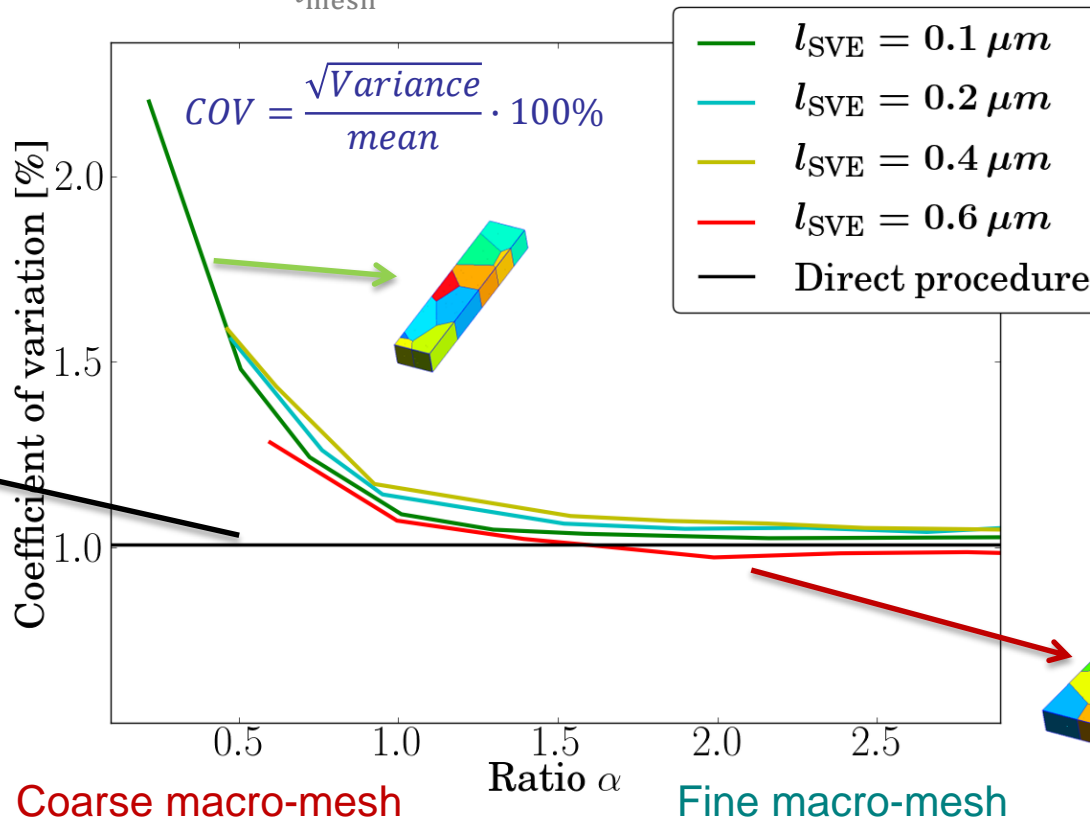
Monte-Carlo simulations at the macro-scale

- Macro-scale beam elements of size l_{mesh}

- Convergence in terms of $\alpha = \frac{l_{Ex}}{l_{\text{mesh}}}$

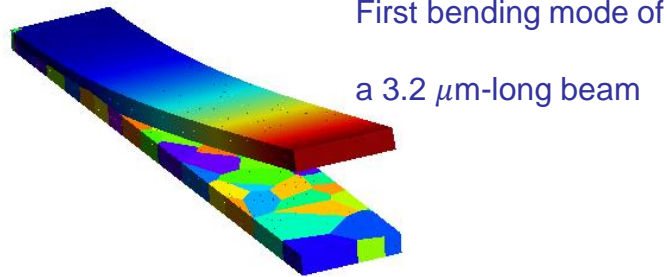


First bending mode of a $3.2 \mu\text{m}$ -long beam

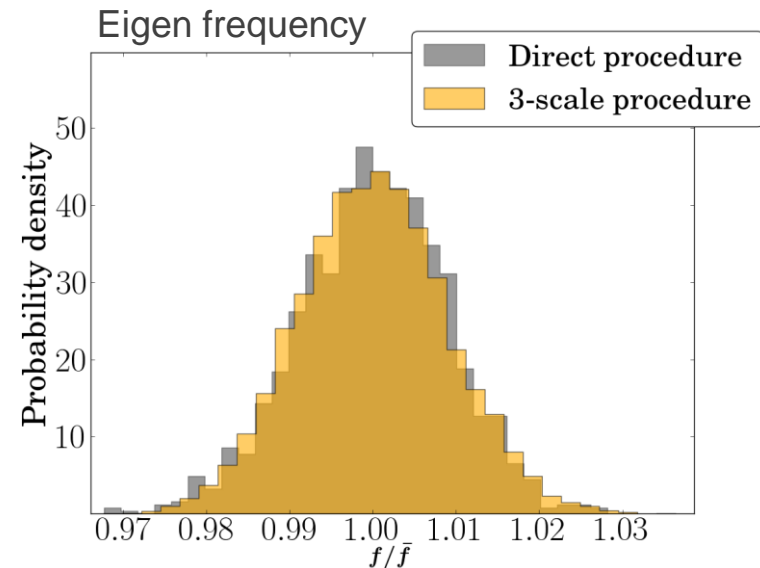
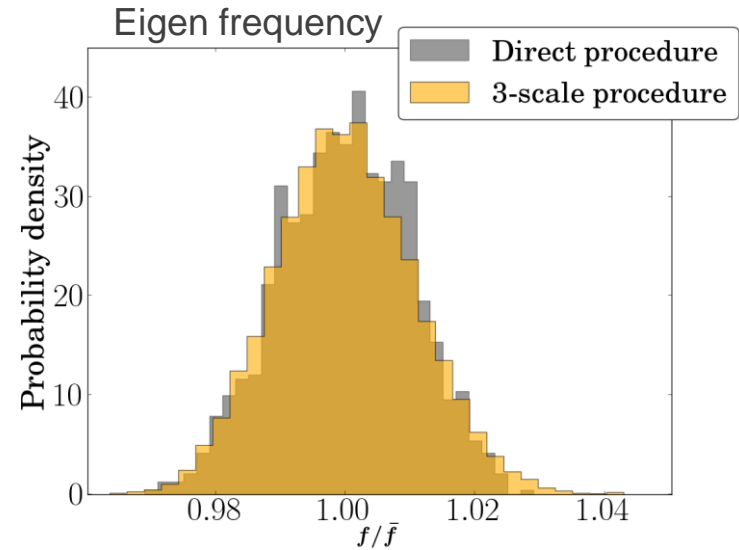
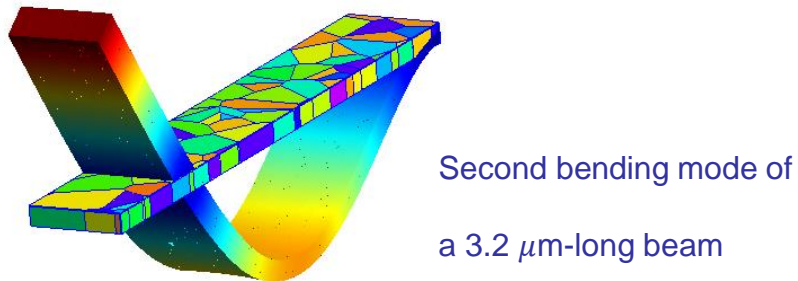


From the meso-scale to the macro-scale

- 3-Scale approach verification ($\alpha \sim 2$) with direct Monte-Carlo simulations
 - First bending mode



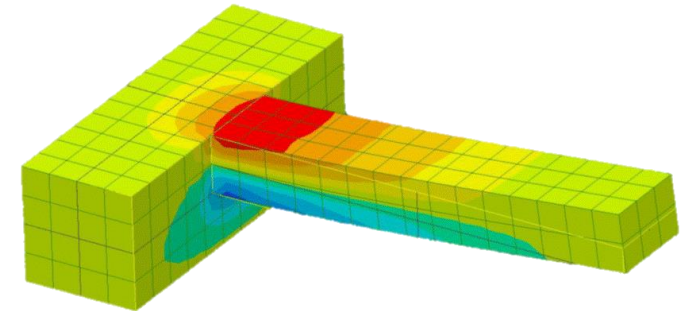
- Second bending mode



- Quality factor

- Micro-resonators

- Temperature changes with compression/traction
 - Energy dissipation



- Eigen values problem

- Governing equations

$$\begin{bmatrix} \mathbf{M} & \mathbf{0} \\ \mathbf{0} & \mathbf{0} \end{bmatrix} \begin{bmatrix} \ddot{\mathbf{u}} \\ \ddot{\boldsymbol{\vartheta}} \end{bmatrix} + \begin{bmatrix} \mathbf{0} & \mathbf{0} \\ \mathbf{D}_{u\boldsymbol{\vartheta}}(\boldsymbol{\theta}) & \mathbf{D}_{\boldsymbol{\vartheta}\boldsymbol{\vartheta}} \end{bmatrix} \begin{bmatrix} \dot{\mathbf{u}} \\ \dot{\boldsymbol{\vartheta}} \end{bmatrix} + \begin{bmatrix} \mathbf{K}_{uu}(\boldsymbol{\theta}) & \mathbf{K}_{u\boldsymbol{\vartheta}}(\boldsymbol{\theta}) \\ \mathbf{0} & \mathbf{K}_{\boldsymbol{\vartheta}\boldsymbol{\vartheta}}(\boldsymbol{\theta}) \end{bmatrix} \begin{bmatrix} \mathbf{u} \\ \boldsymbol{\vartheta} \end{bmatrix} = \begin{bmatrix} \mathbf{F}_u \\ \mathbf{F}_{\boldsymbol{\vartheta}} \end{bmatrix}$$

- Free vibrating problem

$$\begin{bmatrix} \mathbf{u}(t) \\ \boldsymbol{\vartheta}(t) \end{bmatrix} = \begin{bmatrix} \mathbf{u}_0 \\ \boldsymbol{\vartheta}_0 \end{bmatrix} e^{i\omega t}$$

$$\hookrightarrow \begin{bmatrix} -\mathbf{K}_{uu}(\boldsymbol{\theta}) & -\mathbf{K}_{u\boldsymbol{\vartheta}}(\boldsymbol{\theta}) & \mathbf{0} \\ \mathbf{0} & -\mathbf{K}_{\boldsymbol{\vartheta}\boldsymbol{\vartheta}}(\boldsymbol{\theta}) & \mathbf{0} \\ \mathbf{0} & \mathbf{0} & \mathbf{I} \end{bmatrix} \begin{bmatrix} \mathbf{u} \\ \boldsymbol{\vartheta} \\ \dot{\mathbf{u}} \end{bmatrix} = i\omega \begin{bmatrix} \mathbf{0} & \mathbf{0} & \mathbf{M} \\ \mathbf{D}_{\boldsymbol{\vartheta}u}(\boldsymbol{\theta}) & \mathbf{D}_{\boldsymbol{\vartheta}\boldsymbol{\vartheta}} & \mathbf{0} \\ \mathbf{I} & \mathbf{0} & \mathbf{0} \end{bmatrix} \begin{bmatrix} \mathbf{u} \\ \boldsymbol{\vartheta} \\ \dot{\mathbf{u}} \end{bmatrix}$$

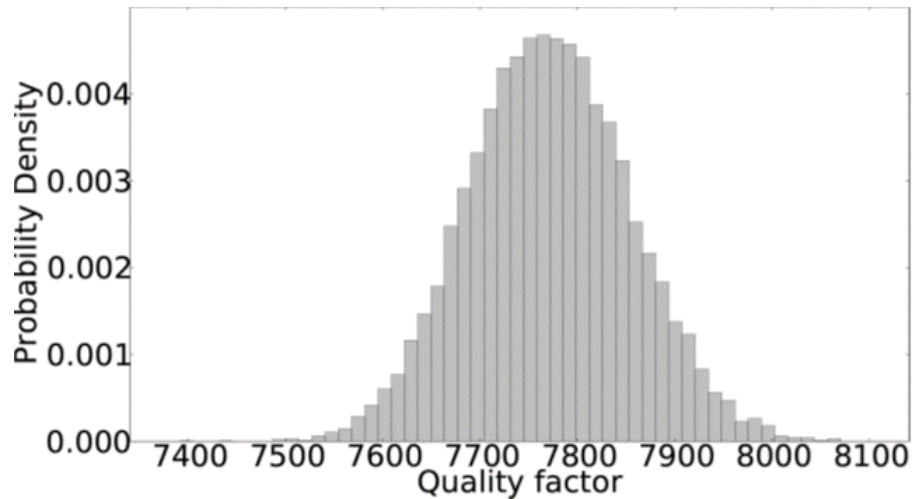
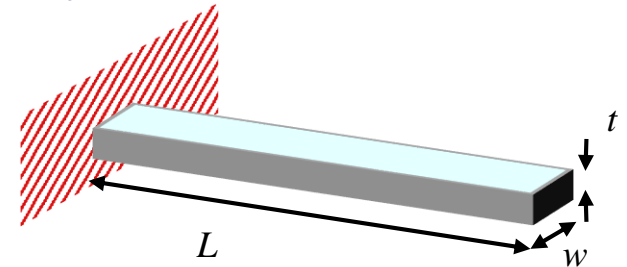
- Quality factor

- From the dissipated energy per cycle

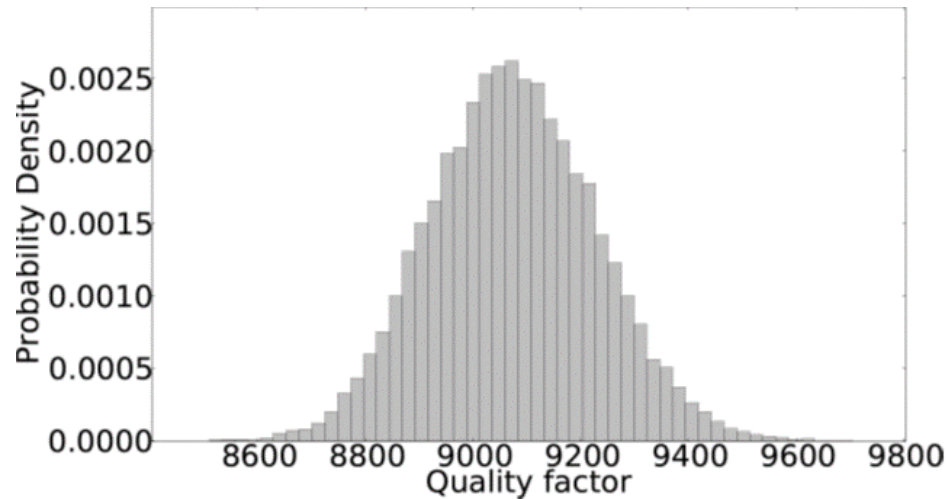
- $$Q^{-1} = \frac{2|\Im\omega|}{\sqrt{(\Re\omega)^2 + (\Im\omega)^2}}$$

From the meso-scale to the macro-scale

- Application of the 3-Scale method to extract the quality factor distribution
 - Perfectly clamped micro-resonator
 - Different sizes easily considered
 - Meso-scale random fields
 - From stochastic homogenization
 - Generated for different deposition temperatures
 - Effect of the deposition temperature



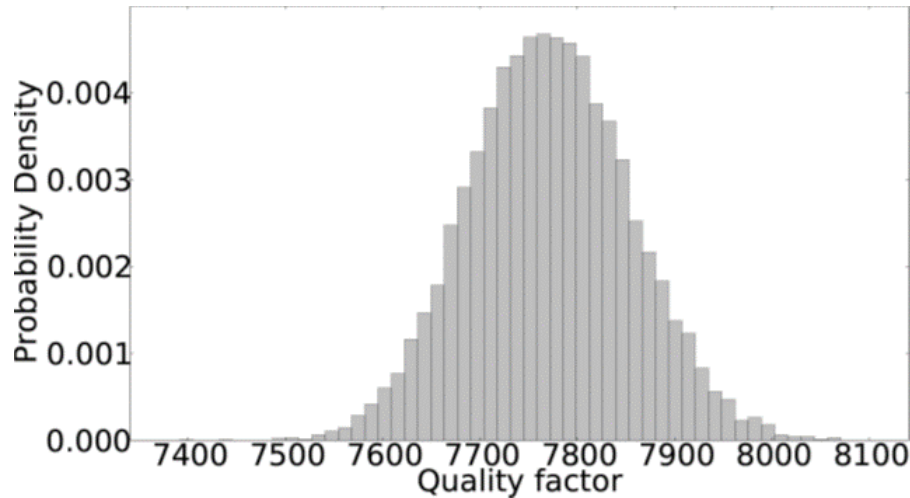
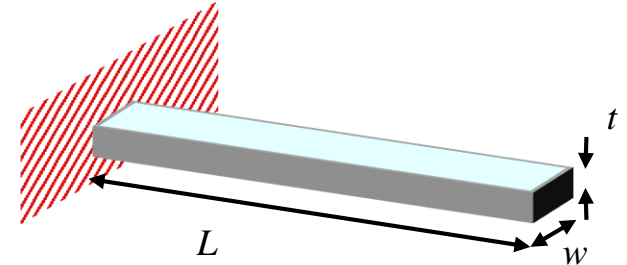
15 x 3 x 2 μm^3 -beam,
deposited at 610 °C



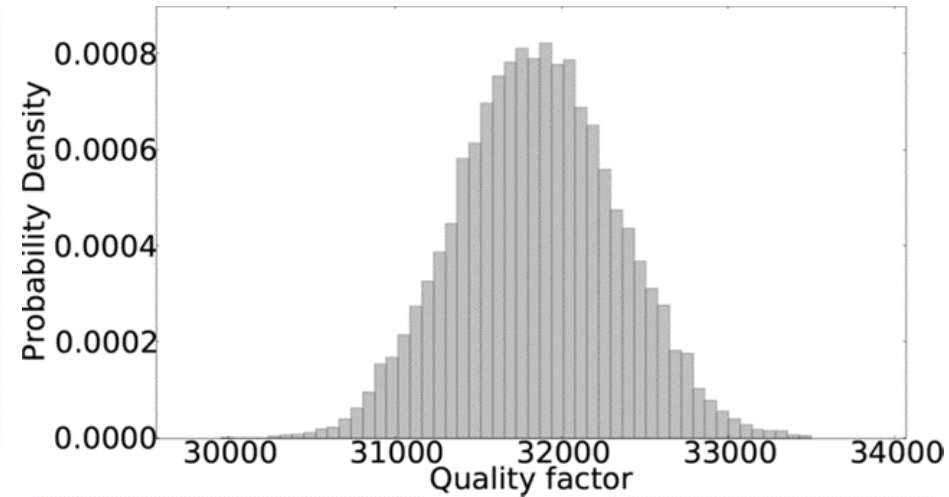
15 x 3 x 2 μm^3 -beam,
deposited at 630 °C

From the meso-scale to the macro-scale

- Application of the 3-Scale method to extract the quality factor distribution (2)
 - Perfectly clamped micro-resonator
 - Effect of the geometry



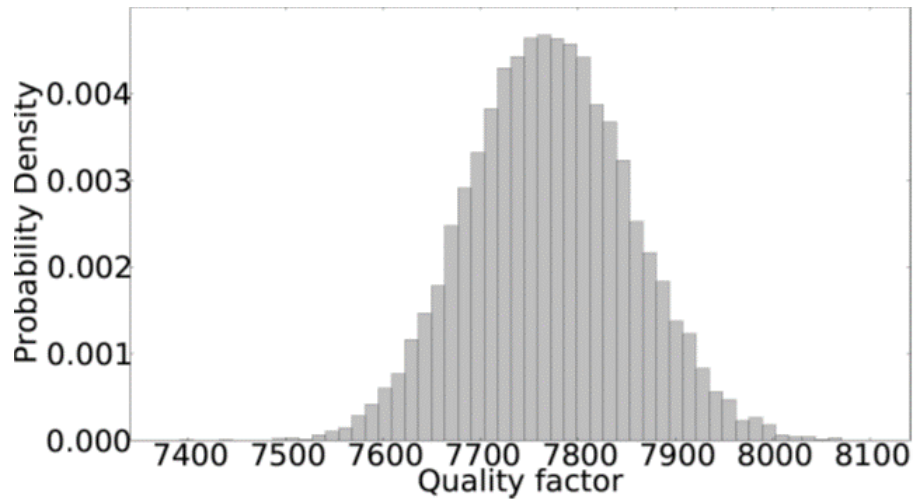
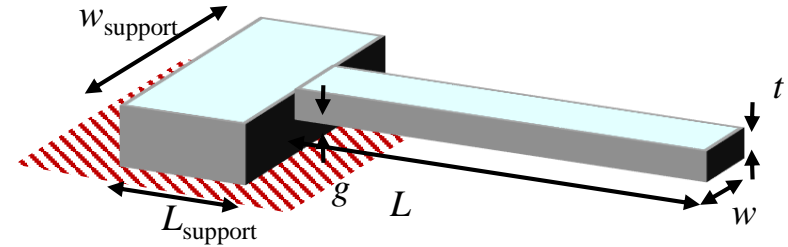
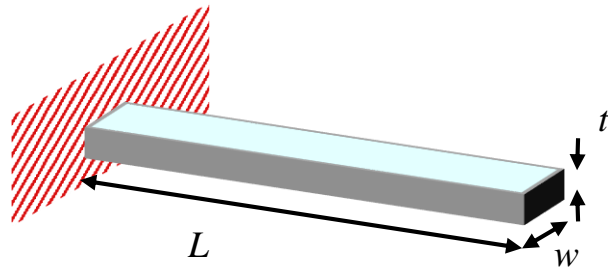
$15 \times 3 \times 2 \mu\text{m}^3$ -beam,
deposited at $610 \text{ }^\circ\text{C}$



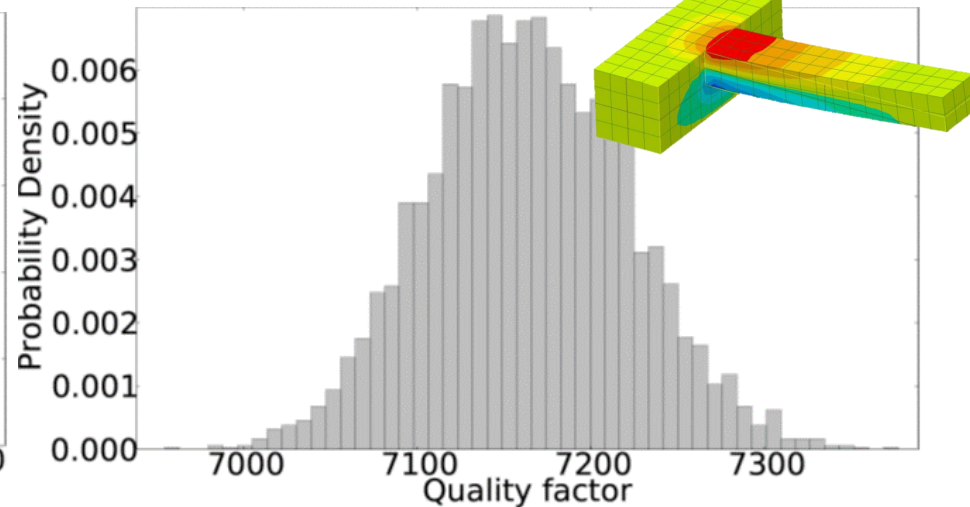
$15 \times 3 \times 1 \mu\text{m}^3$ -beam,
deposited at $610 \text{ }^\circ\text{C}$

From the meso-scale to the macro-scale

- Application of the 3-Scale method to extract the quality factor distribution (3)
 - 3D models readily available
 - The effect of the anchor can be studied



15 x 3 x 2 μm^3 -beam,
deposited at 610 °C

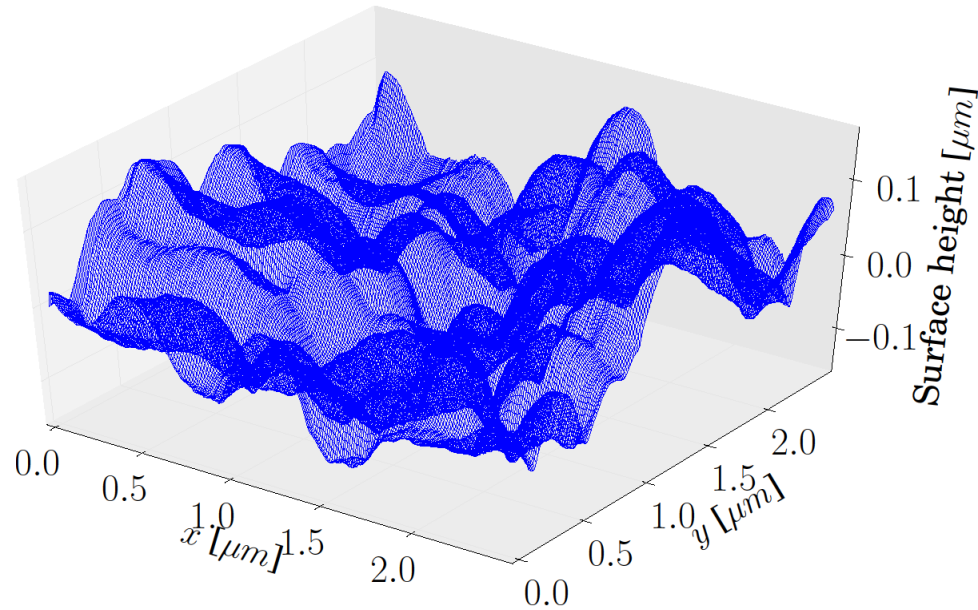


15 x 3 x 2 μm^3 -beam & anchor,
deposited at 610 °C

- Thermo-mechanical problems
 - Governing equations
 - Macro-scale stochastic finite element
 - Meso-scale volume elements
- From the micro-scale to the meso-scale
 - Thermo-mechanical homogenization
 - Definition of Stochastic Volume Elements (SVEs) & Stochastic homogenization
 - Need for a meso-scale random field
- The meso-scale random field
 - Definition of the thermo-mechanical meso-scale random field
 - Stochastic model of the random field: Spectral generator & non-Gaussian mapping
- From the meso-scale to the macro-scale
 - 3-Scale approach verification
 - Application to extract the quality factor
- **Extension to stochastic-plate finite elements**
 - Second-order stochastic homogenization
 - Rough Stochastic Volume Elements
 - Topology uncertainties effects

Extension to stochastic-plate finite elements

- How to account for the surface topology uncertainties?
 - Upper surface topology by AFM measurements on 2 μm -thick poly-silicon films



| | | | | |
|------------------------------------|------|------|------|------|
| Temperature [$^{\circ}\text{C}$] | 580 | 610 | 630 | 650 |
| Std deviation [nm] | 35.6 | 60.3 | 90.7 | 88.3 |

AFM data provided by IMT Bucharest, Rodica Voicu, Angela Baracu, Raluca Muller

Stochastic multi-scale method for Kirchhoff-Love (KL) plates

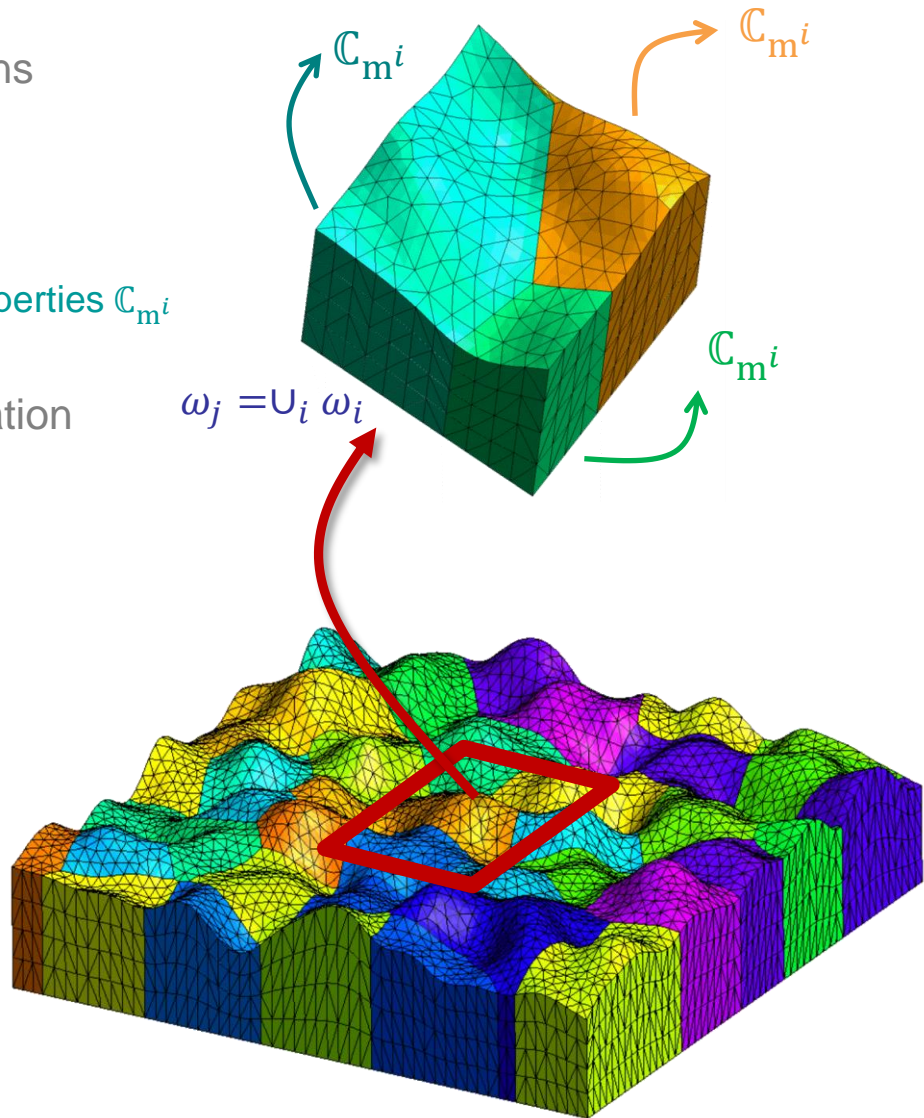
- Rough Stochastic Volume Element

- Poisson Voronoï tessellation realizations
 - From topology generator
 - Use of AFM measurements
- Extraction of volume elements ω_j
 - Each grain ω_i is assigned material properties \mathbb{C}_{m^i}
 - Defined from silicon crystal properties
- Each \mathbb{C}_{m^i} is assigned a random orientation
 - Uniformly distributed
 - Following XRD distributions
- Governing equations
 - Classical continuum mechanics

$$\left\{ \begin{array}{l} \nabla \cdot \boldsymbol{\sigma}_m = 0 \\ \boldsymbol{\varepsilon}_{mij} = \frac{\mathbf{u}_{m^i,j} + \mathbf{u}_{m^j,i}}{2} \end{array} \right.$$

- Anisotropic grains

$$\boldsymbol{\sigma}_m^i = \mathbb{C}_{m^i} : \boldsymbol{\varepsilon}_m^i$$



Stochastic multi-scale method for Kirchhoff-Love (KL) plates

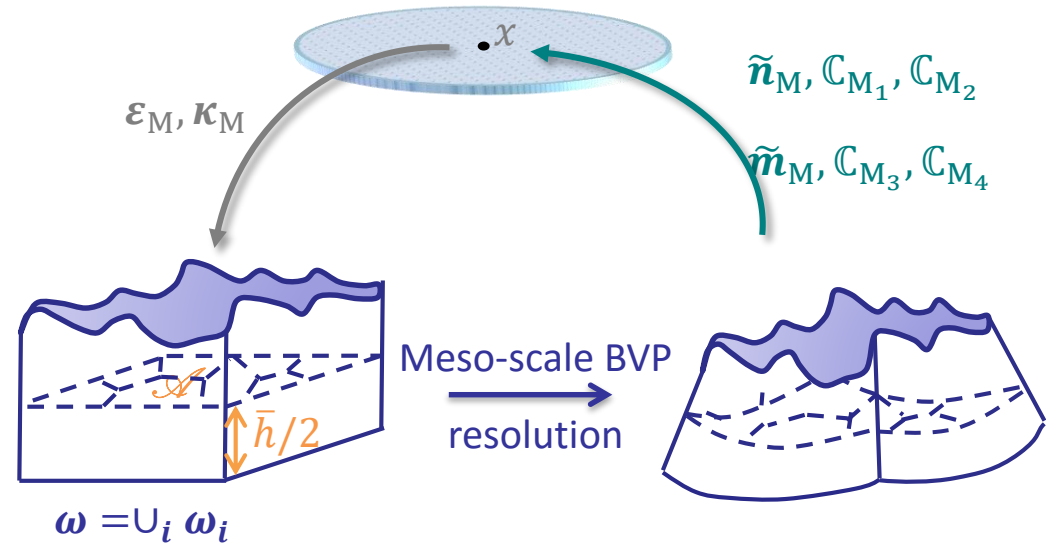
- Second-order homogenization

- Upscaling

$$\begin{cases} \tilde{\mathbf{n}}_M = \mathbb{C}_{M_1} : \boldsymbol{\varepsilon}_M + \mathbb{C}_{M_2} : \boldsymbol{\kappa}_M \\ \tilde{\mathbf{m}}_M = \mathbb{C}_{M_3} : \boldsymbol{\varepsilon}_M + \mathbb{C}_{M_4} : \boldsymbol{\kappa}_M \end{cases}$$

- Stochastic homogenization

- Several SVE realizations
 - For each SVE $\omega_j = U_i \omega_i$



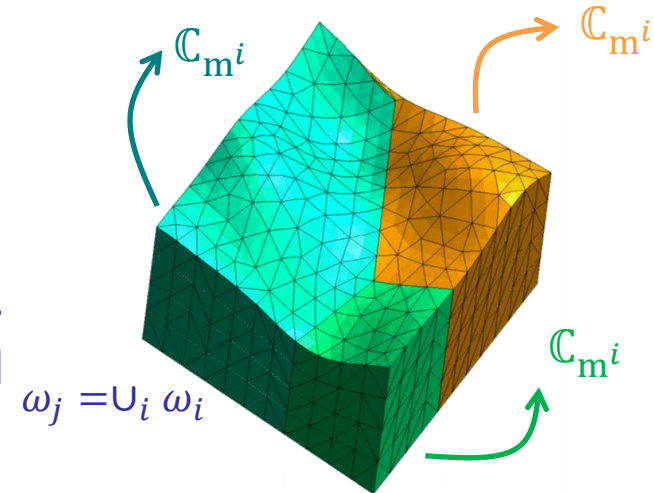
$\mathbb{C}_{m^i} \forall i$

Computational homogenization

$\mathbb{C}_{M_1^j}, \mathbb{C}_{M_2^j}, \mathbb{C}_{M_3^j}, \mathbb{C}_{M_4^j}$

Samples of the meso-scale homogenized elasticity tensors

$\bar{\rho}_{M^j}$



- The density per unit area is now non-constant

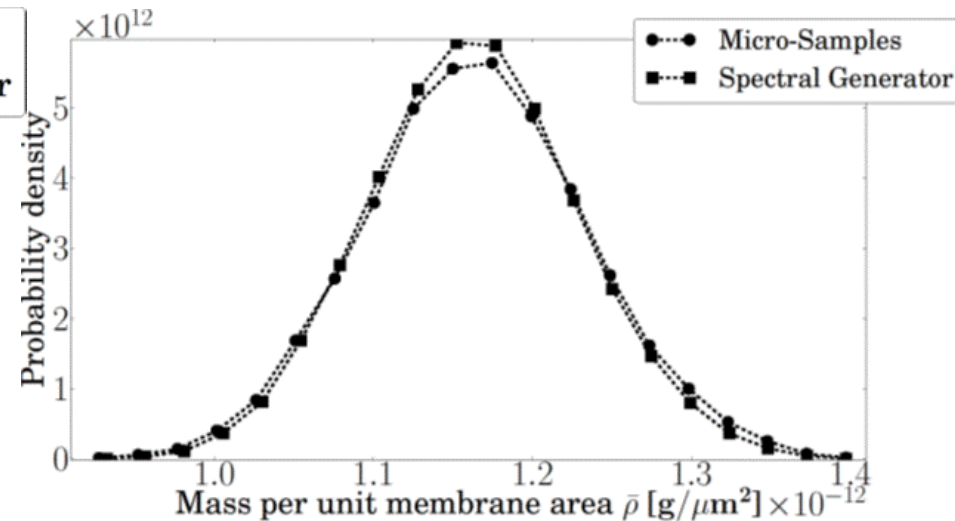
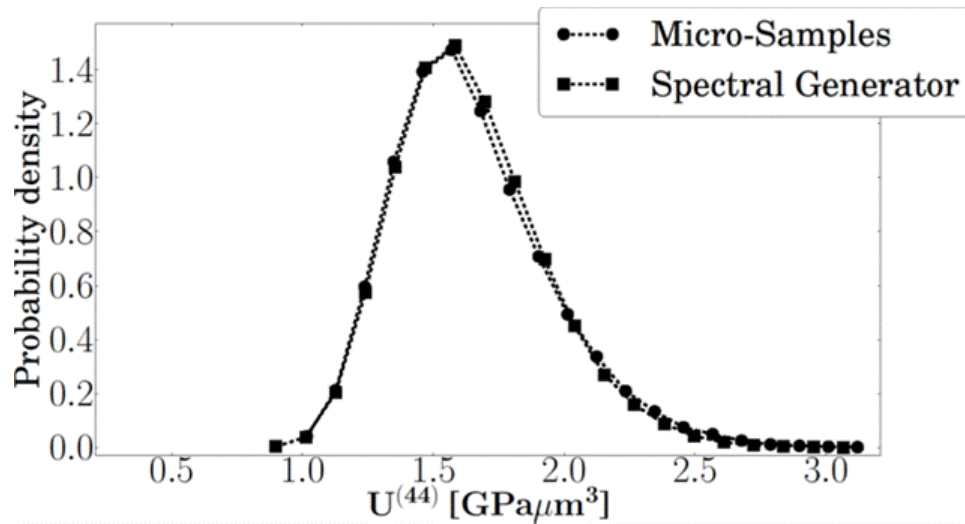
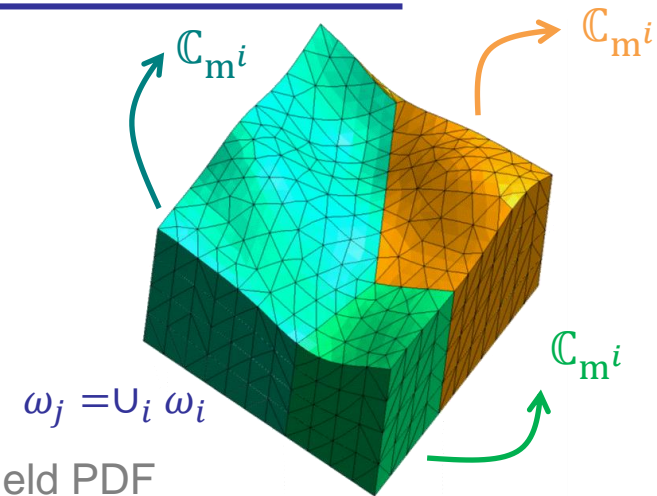
The meso-scale random field

- Generator of meso-scale random fields

- Spectral generator &
- Non-Gaussian mapping

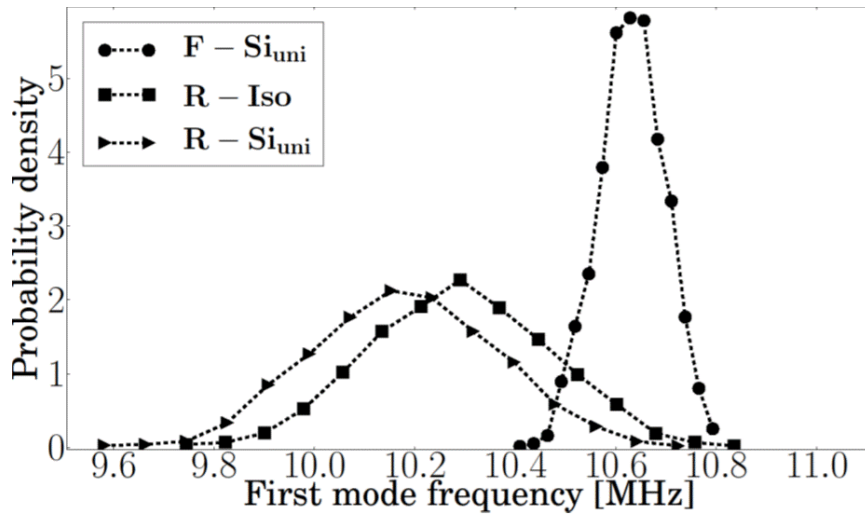
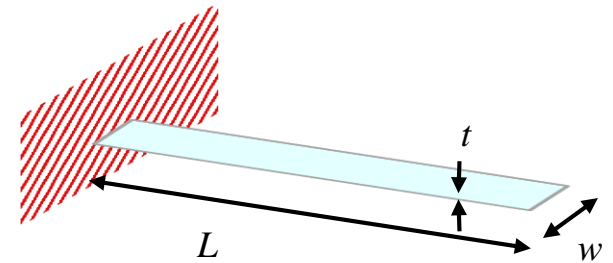
- Polysilicon film deposited at 610 °C

- SVE size of $0.5 \times 0.5 \times 0.5 \mu\text{m}^3$
- Comparison between micro-samples and generated field PDF

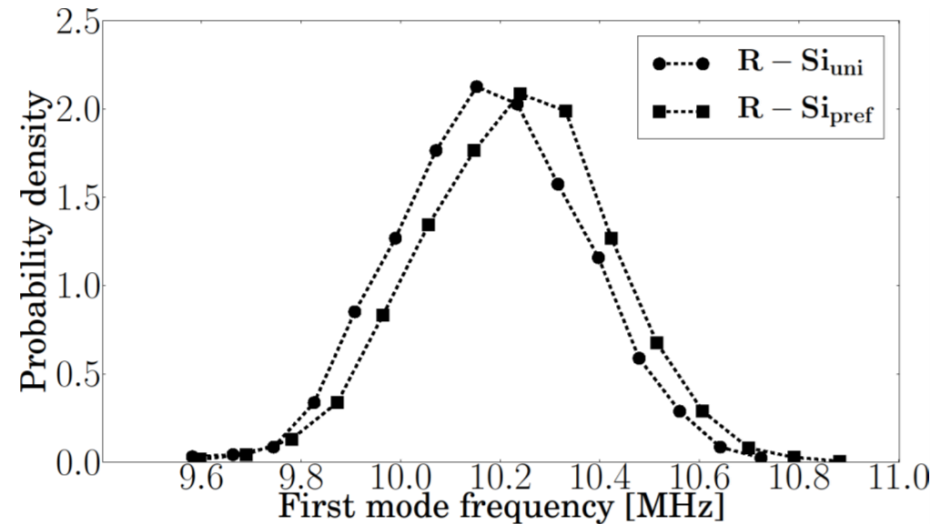


Topology uncertainties effects

- Polysilicon film deposited at 610 °C
 - Cantilever of $8 \times 3 \times 0.5 \mu\text{m}^3$
 - SVE size of $0.5 \times 0.5 \times 0.5 \mu\text{m}^3$



Roughness effect is the most important for $8 \times 3 \times 0.5 \mu\text{m}^3$ cantilevers

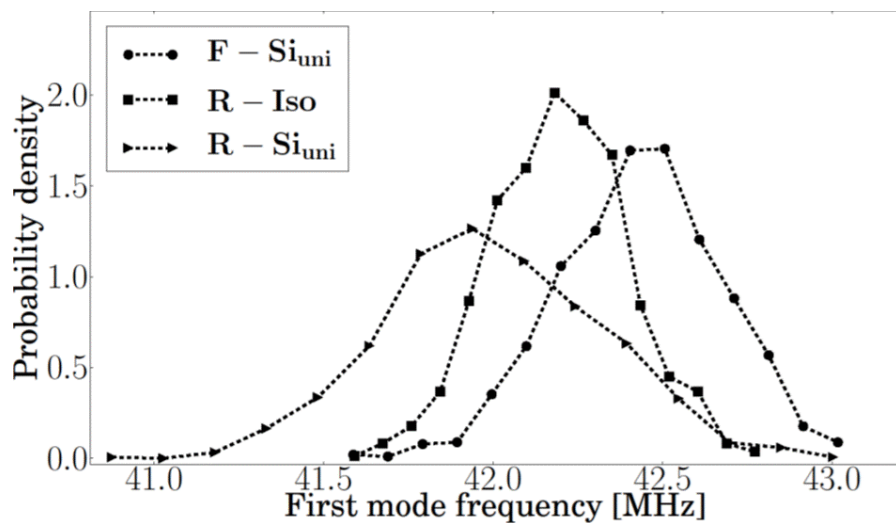
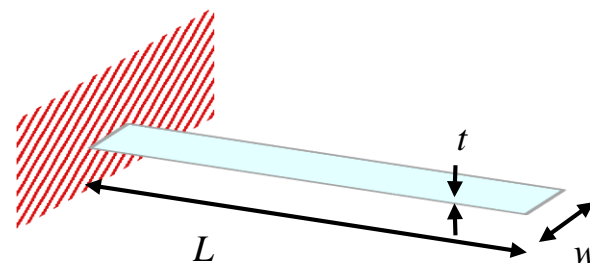


Grain orientation distribution effect for $8 \times 3 \times 0.5 \mu\text{m}^3$ cantilevers

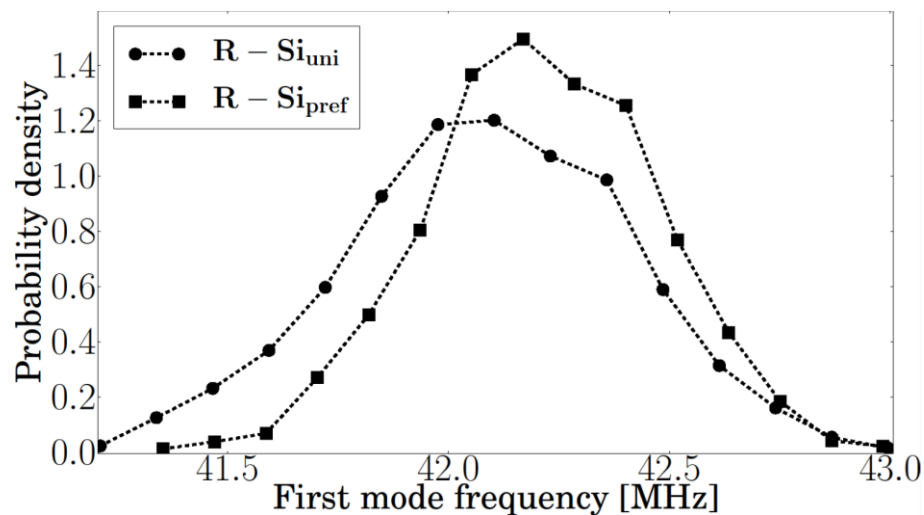
- Flat SVEs (no roughness) - F
- Rough SVEs (Polysilicon film deposited at 610 °C) - R
- Grain orientation following XRD measurements – Si_{pref}
- Grain orientation uniformly distributed – Si_{uni}
- Reference isotropic material – Iso

Topology uncertainties effects

- Polysilicon film deposited at 610 °C
 - Cantilever of $8 \times 3 \times 2 \mu\text{m}^3$
 - SVE size of $0.5 \times 0.5 \times 2 \mu\text{m}^3$



Roughness effect is of same importance as orientation for $8 \times 3 \times 2 \mu\text{m}^3$ cantilevers



Grain orientation distribution effect for $8 \times 3 \times 2 \mu\text{m}^3$ cantilevers

- **Efficient stochastic multi-scale method**
 - Micro-structure based on experimental measurements
 - Computational efficiency rely on the meso-scale random field generator
 - Used to study probabilistic behaviors

- **Perspectives**
 - Other material systems
 - Non-linear behaviors
 - Non-homogenous random fields

Thank you for your attention !

- Macro-scale Kirchhoff-Love plates

- Displacement fields
 - Displacement \mathbf{u} of Cosserat plane, and
 - Cross section direction \mathbf{t} with

$$\Delta \mathbf{t}_\alpha = -\mathbf{u}_{z,\alpha}$$

- Kinematics: in-plane strain and curvature

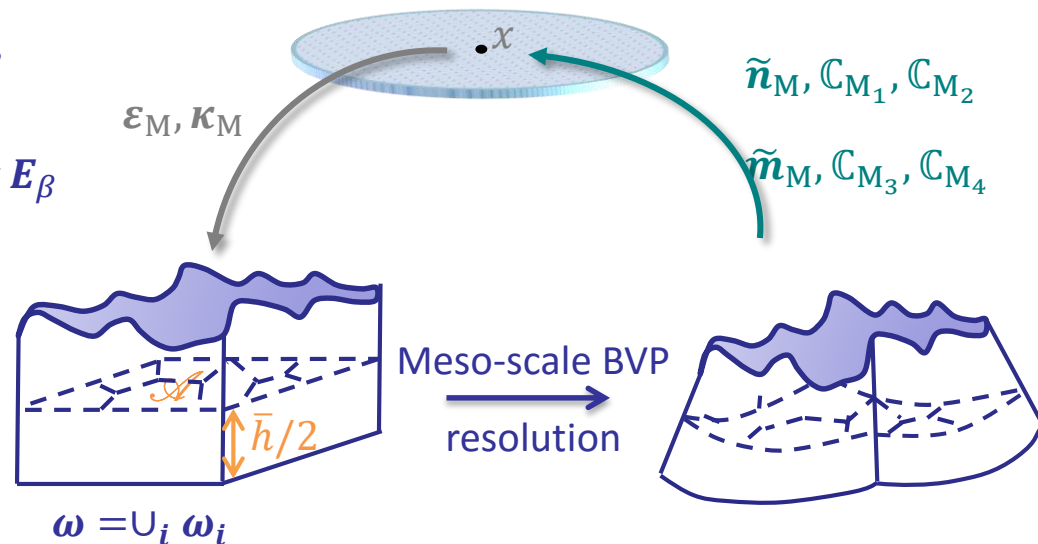
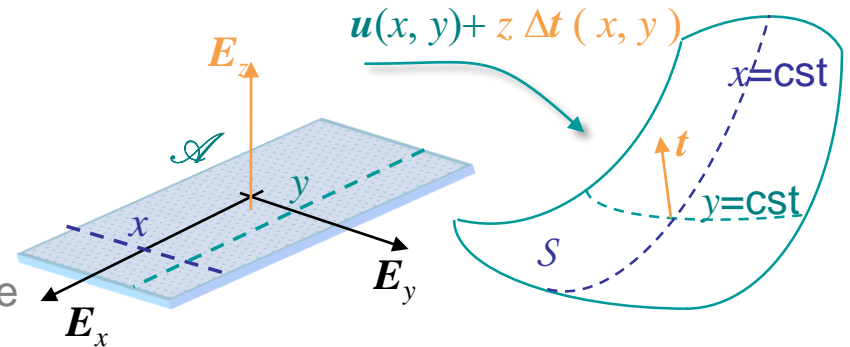
$$\left\{ \begin{array}{l} \boldsymbol{\varepsilon}_{M\alpha\beta} = \frac{\mathbf{u}_{\beta,\alpha} + \mathbf{u}_{\alpha,\beta}}{2} \\ \boldsymbol{\kappa}_{M\alpha\beta} = \frac{\Delta \mathbf{t}_{\beta,\alpha} + \Delta \mathbf{t}_{\alpha,\beta}}{2} = -\mathbf{u}_{z,\alpha\beta} \end{array} \right.$$

- Resultant in-plane & bending stresses

$$\left\{ \begin{array}{l} \mathbf{n}_M^\alpha = \tilde{\mathbf{n}}_M^{\alpha\beta} \mathbf{E}_\beta = \int_h \boldsymbol{\sigma}_M^{\alpha\beta} dz \mathbf{E}_\beta \\ \tilde{\mathbf{m}}_M^\alpha = \tilde{\mathbf{m}}_M^{\alpha\beta} \mathbf{E}_\beta = \int_h \boldsymbol{\sigma}_M^{\alpha\beta} z dz \mathbf{E}_\beta \end{array} \right.$$

- Constitutive laws

$$\left\{ \begin{array}{l} \tilde{\mathbf{n}}_M = \mathbb{C}_{M_1} : \boldsymbol{\varepsilon}_M + \mathbb{C}_{M_2} : \boldsymbol{\kappa}_M \\ \tilde{\mathbf{m}}_M = \mathbb{C}_{M_3} : \boldsymbol{\varepsilon}_M + \mathbb{C}_{M_4} : \boldsymbol{\kappa}_M \end{array} \right.$$



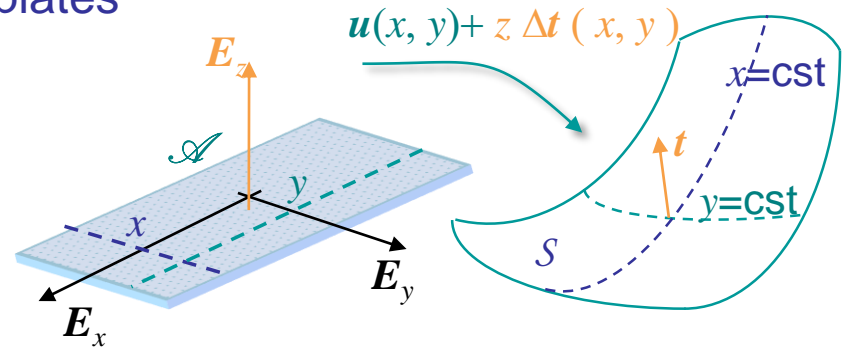
Extension to stochastic-plate finite elements

- Stochastic macro-scale Kirchhoff-Love plates

- Strong form:

$$\left\{ \begin{array}{l} \bar{\rho}_M \ddot{\mathbf{u}} + (\mathbf{n}_M^\alpha)_{,\alpha} = 0 \\ I_{PM} \ddot{\mathbf{t}} + (-\lambda \mathbf{E}_z) + (\tilde{\mathbf{m}}_M^\alpha)_{,\alpha} = 0 \end{array} \right.$$

with $\Delta \mathbf{t}_\alpha = -\mathbf{u}_{z,\alpha}$



- Constitutive equations & density per unit area from stochastic homogenization

$$\left\{ \begin{array}{l} \tilde{\mathbf{n}}_M = \mathbb{C}_{M_1}(\mathbf{x}, \boldsymbol{\theta}) : \boldsymbol{\varepsilon}_M + \mathbb{C}_{M_2}(\mathbf{x}, \boldsymbol{\theta}) : \boldsymbol{\kappa}_M \\ \tilde{\mathbf{m}}_M = \mathbb{C}_{M_3}(\mathbf{x}, \boldsymbol{\theta}) : \boldsymbol{\varepsilon}_M + \mathbb{C}_{M_4}(\mathbf{x}, \boldsymbol{\theta}) : \boldsymbol{\kappa}_M \\ \bar{\rho}_M(\mathbf{x}, \boldsymbol{\theta}) \end{array} \right. \quad \text{with} \quad \left\{ \begin{array}{l} \boldsymbol{\varepsilon}_{M_{\alpha\beta}} = \frac{\mathbf{u}_{\beta,\alpha} + \mathbf{u}_{\alpha,\beta}}{2} \\ \boldsymbol{\kappa}_{M_{\alpha\beta}} = \frac{\Delta \mathbf{t}_{\beta,\alpha} + \Delta \mathbf{t}_{\alpha,\beta}}{2} = -\mathbf{u}_{z,\alpha\beta} \end{array} \right.$$

- Stochastic (Discontinuous Galerkin) finite elements

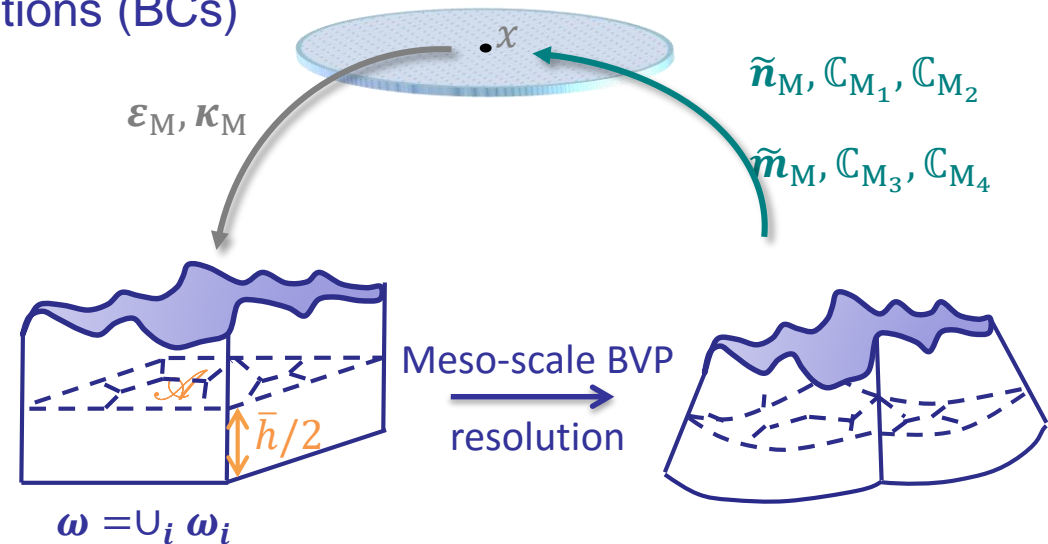
$$\hookrightarrow \mathbf{M}(\boldsymbol{\theta}) \ddot{\mathbf{u}} + \mathbf{K}_{uu}(\boldsymbol{\theta}) \mathbf{u} = \mathbf{F}$$

Second-order stochastic homogenization

- Meso-scale BVP boundary conditions (BCs)

- Downscaling

$$\left\{ \begin{array}{l} \boldsymbol{\varepsilon}_M = \frac{1}{V(\omega)} \int_{\omega} \boldsymbol{\varepsilon}_m d\omega \\ \boldsymbol{\eta}_M \text{ independent of BC} \end{array} \right.$$



- Meso-scale BVP fluctuation field

$$\hookrightarrow \mathbf{u}_m = \boldsymbol{\varepsilon}_M \otimes \mathbf{x} + \frac{1}{2} \boldsymbol{\eta}_M : (\mathbf{x} \otimes \mathbf{x}) + \mathbf{u}' \quad \longrightarrow \quad \left\{ \begin{array}{l} 0 = \int_{\partial\omega} \mathbf{u}' \otimes \mathbf{n} d\partial\omega \\ 0 = \int_{\partial\omega} \mathbf{u}' \otimes \mathbf{n} \otimes \mathbf{x} d\partial\omega \end{array} \right.$$

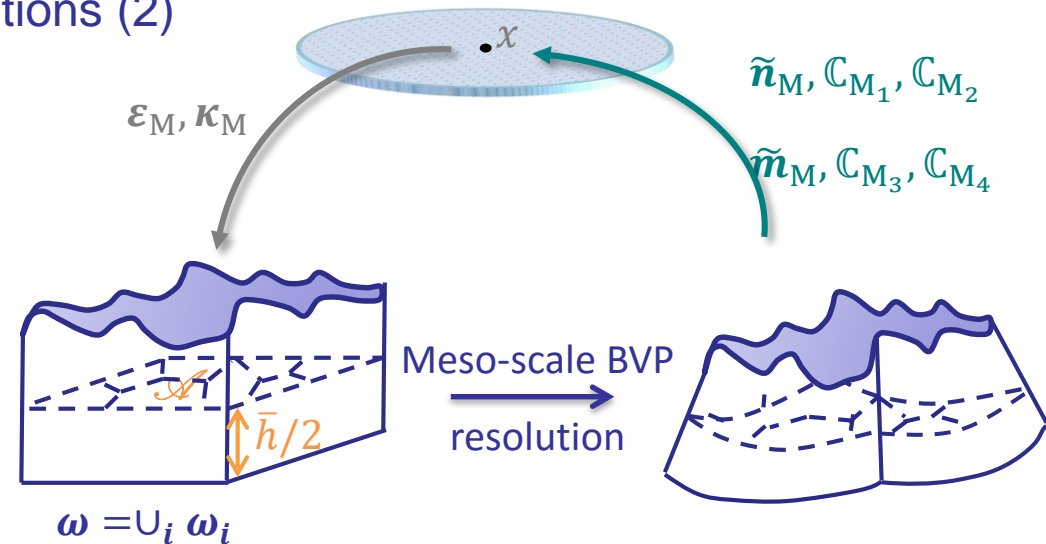
→ $\left\{ \begin{array}{l} \text{Satisfied by periodic and kinematic boundary conditions} \\ \text{First equation satisfied by static boundary conditions} \end{array} \right.$

Second-order stochastic homogenization

- Meso-scale BVP boundary conditions (2)

- Upscaling

$$\left\{ \begin{array}{l} \mathbf{n}_M = \frac{1}{S} \int_{\omega} \boldsymbol{\sigma}_m d\omega \\ \mathbf{m}_M = \frac{1}{S} \int_{\omega} \boldsymbol{\sigma}_m \otimes \mathbf{x} d\omega \end{array} \right.$$



- Consistency

$$\hookrightarrow \mathbf{n}_M : \delta \boldsymbol{\varepsilon}_M + \mathbf{m}_M : \delta \boldsymbol{\eta}_M = \frac{1}{S} \int_{\omega} \boldsymbol{\sigma}_m : \delta \boldsymbol{\varepsilon}_m d\omega \longrightarrow 0 = \int_{\partial \omega} (\boldsymbol{\sigma}_m \cdot \mathbf{n}) \cdot \mathbf{u}' d\partial \omega$$

\longrightarrow Satisfied by periodic, kinematic, static boundary conditions

- Top and bottom surfaces

- Stress free \longrightarrow plane stress is naturally ensured

- Side surfaces

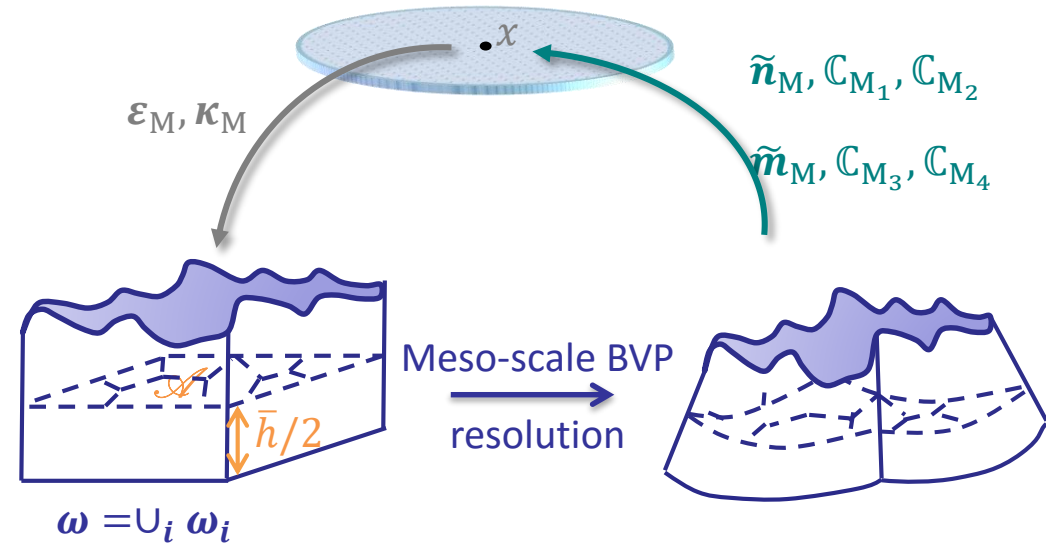
- Mixed boundary conditions

- Second-order homogenization

- Downscaling

$$\left\{ \begin{aligned} \boldsymbol{\epsilon}_M &= \mathbf{u}_M \otimes \nabla \\ &= \boldsymbol{\epsilon}_M^{\alpha\beta} \mathbf{E}_\alpha \otimes \mathbf{E}_\beta + \hat{\boldsymbol{\epsilon}}_M \\ \boldsymbol{\eta}_M &= \mathbf{u}_M \otimes \nabla \otimes \nabla \\ &= \boldsymbol{\kappa}_M^{\alpha\beta} \mathbf{E}_\alpha \otimes \mathbf{E}_\beta \otimes \mathbf{E}_z + \hat{\boldsymbol{\eta}}_M \end{aligned} \right.$$

- $\hat{\boldsymbol{\epsilon}}_M$ & $\hat{\boldsymbol{\eta}}_M$ undefined for KL plates



- Upscaling

$$\left\{ \begin{aligned} \mathbf{n}_M &= \frac{1}{S} \int_{\omega} \boldsymbol{\sigma}_m d\omega = \tilde{\mathbf{n}}_M^{\alpha\beta} \mathbf{E}_\beta \otimes \mathbf{E}_\beta + \hat{\mathbf{n}}_M \\ \mathbf{m}_M &= \frac{1}{S} \int_{\omega} \boldsymbol{\sigma}_m \otimes \mathbf{x} d\omega = \tilde{\mathbf{m}}_M^{\alpha\beta} \mathbf{E}_\beta \otimes \mathbf{E}_\beta \otimes \mathbf{E}_z + \hat{\mathbf{m}}_M \end{aligned} \right.$$

- $\hat{\mathbf{n}}_M = 0$ & $\hat{\mathbf{m}}_M = 0$ for KL plates

↳ $\hat{\boldsymbol{\epsilon}}_M$ & $\hat{\boldsymbol{\eta}}_M$ eliminated →

$$\left\{ \begin{aligned} \tilde{\mathbf{n}}_M &= \mathbb{C}_{M_1} : \boldsymbol{\epsilon}_M + \mathbb{C}_{M_2} : \boldsymbol{\kappa}_M \\ \tilde{\mathbf{m}}_M &= \mathbb{C}_{M_3} : \boldsymbol{\epsilon}_M + \mathbb{C}_{M_4} : \boldsymbol{\kappa}_M \end{aligned} \right.$$